applied sciences

MDPI

Article

Combined Geophysical–Geodynamic Analysis of the Plio-Pleistocene Hominin Dispersal Through the Levantine Corridor

Lev V. Eppelbaum [1,2,*] and Youri I. Katz [3]

[1] Department of Geophysics, Tel Aviv University, Tel Aviv 6997801, Israel
[2] Azerbaijan State Oil and Industry University, 20 Azadlig Ave., Baku AZ1010, Azerbaijan
[3] The Steinhardt Museum of Natural History and National Research Center, Faculty of Life Sciences, Tel Aviv University, Tel Aviv 6997801, Israel; kiyour@mail.ru
* Correspondence: levap@tauex.tau.ac.il

Abstract

The origin of humans on Earth is closely linked to understanding how ancient populations dispersed into adjacent territories. Traditionally, studies have identified landscape and climatic changes as the primary factors in this dispersal. However, we propose that regional tectonic and geodynamic factors also played a significant role in shaping these movements. To analyze this phenomenon, we employed several primary methods, including radiometric dating, magnetostratigraphy, paleomagnetic correlation, isotope–oxygen analysis, tectonothermal studies, gravity mapping, paleobiogeographic assessment, lithofacies analysis, and event and cyclic stratigraphy. Our research indicates that the Akchagylian hydrospheric maximum, which reached up to +200 m, significantly limited the early dispersal of hominins from Africa to Eurasia. The migration corridor was shaped by tectonic activity between the Dead Sea Transform and the boundary of the Mesozoic Terrane Belt carbonate platform. We argue that, during the early stages of hominin evolution in East Africa, the Levantine Corridor (LC) had not yet developed into an optimal route for dispersal, either tectonically or paleogeographically. Suitable habitats for early hominins emerged only after the regression at the end of the Middle Gelasian, around two million years ago, when sea level fell by approximately 200 m, leading to the dissection of the coastal high plateau of the Eastern Mediterranean. We therefore suggest that the LC became established only after the termination of the Akchagylian transgression and the subsequent landscape reconfiguration of the Eastern Mediterranean. Our integrated analysis, combining paleomagnetic, structural, tectonic, and event stratigraphy data, indicates that the age of the renowned 'Ubeidiya site in northern Israel is several hundred thousand years older than previously thought. This paleogeographic impact had not been considered in earlier studies. Considering the diverse and complex factors that governed hominin dispersal from Africa into Eurasia within this multifaceted region, we propose that the scope of research should be broadened. Our detailed study of the Carmel area, located northeast of the Levantine Corridor and influenced by it during the Pleistocene, indicates that this region was inundated during the early phases of hominin migration out of Eastern Africa. Besides this, we have conducted an integrated geological–geophysical landscape analysis of the central part of the Israeli coastal plain.

Keywords: paleomagnetic correlation and dating; gravity mapping; isotope-oxygen analysis; paleogeographic reconstructions; Levantine Corridor; ancient man dispersal

check for updates

Academic Editors: Sabrina Grassi, Sebastiano Imposa and Claudia Pirrotta

Received: 12 September 2025
Revised: 22 October 2025
Accepted: 27 October 2025
Published: 29 October 2025

Citation: Eppelbaum, L.V.; Katz, Y.I. Combined Geophysical–Geodynamic Analysis of the Plio-Pleistocene Hominin Dispersal Through the Levantine Corridor. *Appl. Sci.* **2025**, *15*, 11554. https://doi.org/10.3390/app152111554

Correction Statement: This article has been republished with a minor change. The change does not affect the scientific content of the article and further details are available within the backmatter of the website version of this article.

Copyright: © 2025 by the authors. Licensee MDPI, Basel, Switzerland. This article is an open access article distributed under the terms and conditions of the Creative Commons Attribution (CC BY) license (https://creativecommons.org/licenses/by/4.0/).

1. Introduction

Although climatic and ecological conditions played a role in constraining early hominin dispersal, their explanatory power remains limited, as these features were inherited mainly from the Miocene. They were shaped by equatorial transgressions and the relatively weak development of polar glaciation. One million years ago (1 Ma), the absence of continental glaciation prevented the establishment of strong climatic and ecological zonation. From a paleogeographic perspective, the Akchagylian–Gelasian seas, like those of the Miocene, inundated extensive shelf areas; their hydrospheric maxima rose approximately 200 m above present sea level, and the Paratethys shelf basin remained vast and uniform (Figure 1). Analysis of hydrospheric disturbances further suggests that the meridional asymmetry of the Earth's figure—manifested through polar transgressions, equatorial compression, and continental glaciations—emerged only at the close of the Matuyama epoch, around 844 Kyr ago.

The principal transgressive maximum was recorded on the Eurasian platform, where evidence of the Akchagylian Sea reached elevations of +186 m [1]. A comparable maximum of +180 m was identified on the Epipaleozoic platform of Great Britain [2]. Similar studies have been carried out within the African continental plate in Egypt [3]. Akchagylian–Gelasian ingressions in the Nile erosional valley extended southward to the latitude of Sudan and attained elevations of approximately +200 m. Camps and Chauhan [4] present an analysis of extensive paleomagnetic data in conjunction with paleogeographic reconstructions of the Tethys and Paratethys basins.

The questions concerning the origin and evolutionary traits of ancient hominins, as well as the associated landscape and climatic conditions of habitation, have given rise to numerous methodological and theoretical studies [5–7]. Given that this pivotal dispersal occurred during the Late Cenozoic, it is essential to identify the key geological and geophysical factors that facilitated the emergence and spread of early humans within the transitional zone between Africa and Eurasia [1,8]. In this context, the Eastern Mediterranean represents a critical region through which, according to radiometric and paleomagnetic evidence, hominins dispersed from their primary East African range into Eurasia approximately 1.8–2.5 Ma (Figure 2).

2. Setting of Materials and Methods

To address the challenges of ancient hominin dispersal through the Levantine Corridor, a range of geological, archaeological, and geophysical methods were employed. Among these methods, we can note paleogeographic [2,9,10], archaeological [11–23], geomorphological [4,5,23–25], geophysical (paleomagnetic, gravity, and tectonothermal) [7,10,26–34] (A. Ginzburg's gravity map), paleontological [13,35–41] and palinspastic reconstructions [42], as well as planetary–geodynamic mapping methods [34,43–45] were applied. A wide range of sources on historical planetology, stratigraphy, tectonic–structural frameworks, paleopedology, and ecological–stratigraphic analysis was extensively utilized to compare marine and continental formations [3,8–11,16,17,46–52]. Numerous data on geological mapping were also used [50,53–60].

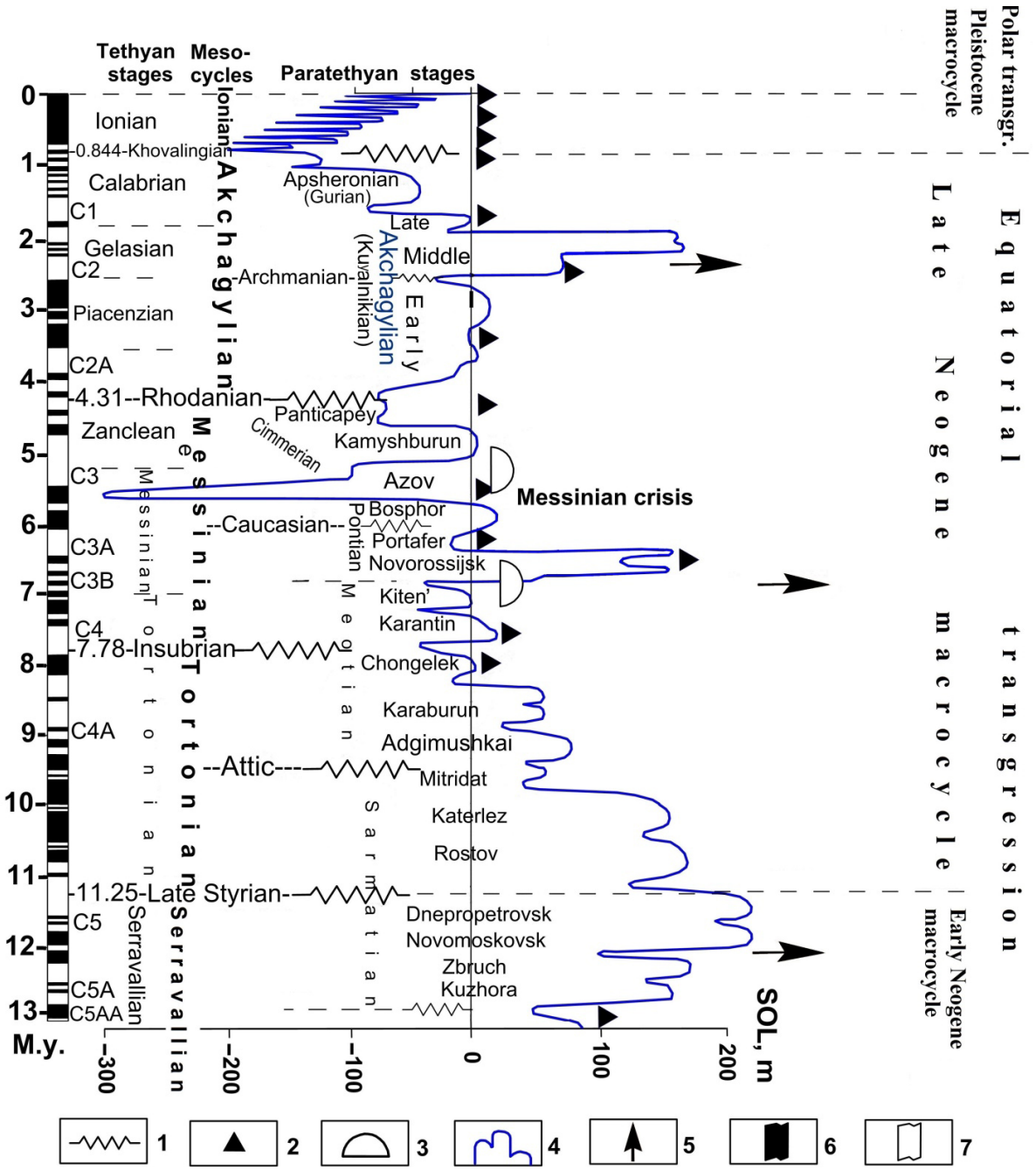


Figure 1. The scheme of hydrospheric disturbances in the Tethyan–Paratethyan in the second half of the Late Cenozoic and their paleomagnetic correlation (revised and supplemented after [1]. (1) tectonic phases, (2) glacial epochs, (3) principal stages of evaporite sedimentation, (4) 'Standard Ocean Level' (SOL) curve, in meters, (5) maxima of positive hydrospheric disturbances, (6) intervals of normal magnetic polarity, (7) intervals of reversed magnetic polarity, (7) magnetic field of reverse polarity. The paleomagnetic data were generalized based on [7,13,17,19,26,31–33,49,61–63].

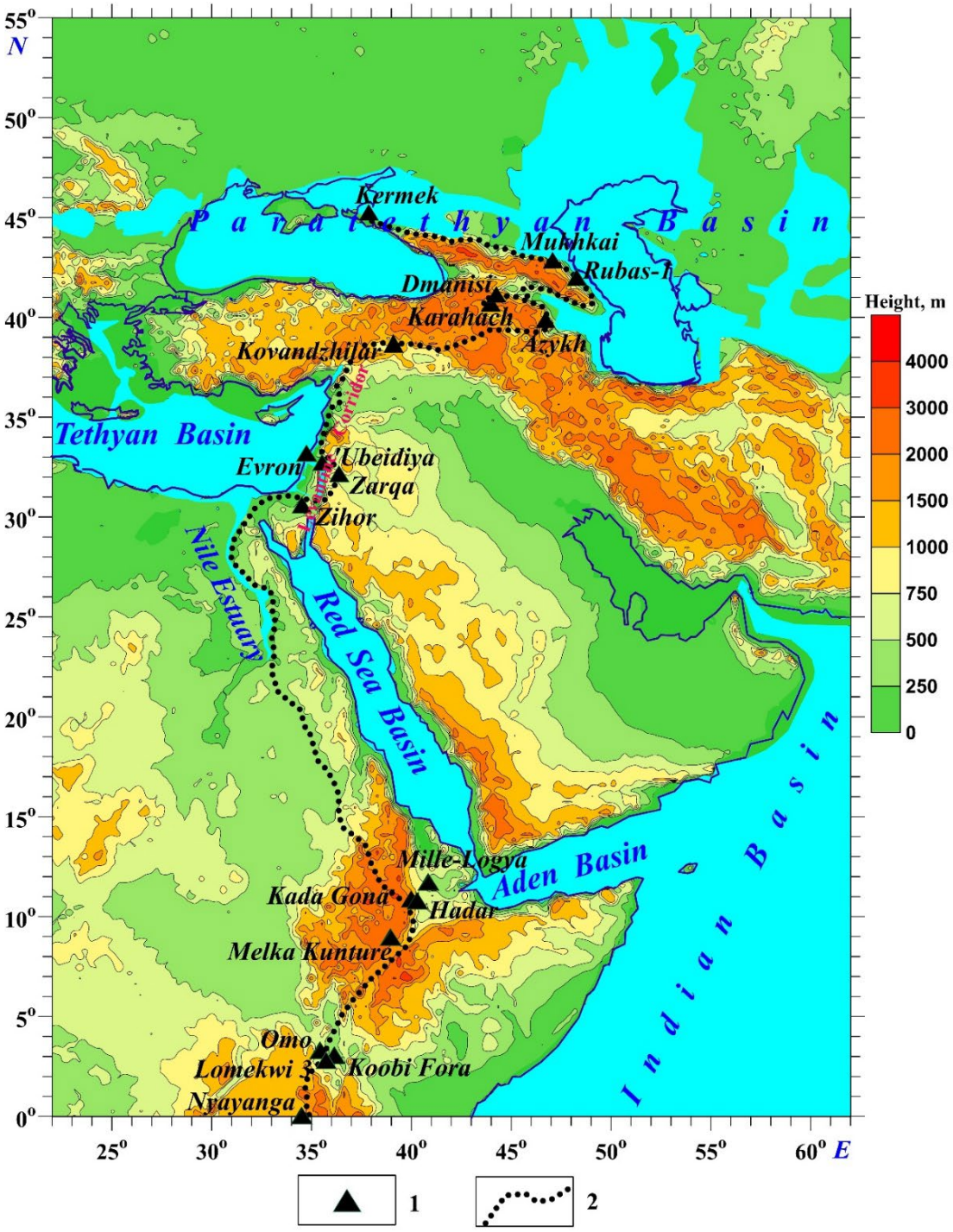


Figure 2. Geomorphological–paleogeographic map of the study area showing the main hydrographic features, current topography, and locations of ancient hominin sites (revised and supplemented from [1]). (1) ancient hominin sites of 3.3–1.77 Ma, (2) reconstructed ancient hominin way from Africa to Eurasia. The age of anthropological sites is taken from: Nyayanga (3.03–2.58 Ma, [64]), Lomekwi (3.3 Ma, [65]), Koobi Fora (2.1–1.6 Ma, [66]), Omo (2.4–2.3 Ma, [67]), Hadar (2.4–2.3 Ma, [68]), Kada Gona (2.6–2.0 Ma, [37]), Mille-Logia (2.42–2.1 Ma, [69]), Zihor (1.95–1.78 Ma, [63]), Zarqa (2.5–1.95 Ma, [19]), 'Ubeidiya (1.8–2.6 Ma, [51]), Kovandzhilar (2.0–1.7 Ma, [70]), Melka Kunture (~ 2.0 Ma, [52]); Azykh (2.1–1.9 Ma, [71]), Karahach (1.85–1.78 Ma, [72]), Dmanisi (1.85–1.77, [73]), Rubas-1 (2.2–2.3 Ma, [74]), Mukhkai (2.1–1.77 Ma, [75]), Kermek (2.1–1.95 Ma, [76]).

3. Results

3.1. Hydrospheric Disturbances in the Earth's Evolution

Hydrospheric disturbances are a significant element in the development of stratigraphic scales (Figure 1). During the last 12 Ma of the Late Cenozoic, there are three hydrospheric maxima with a height of about +200 m—Early Sarmatian, Early Pontic, and Middle Akchagylian, and two minima—the Late Messinian–Early Pliocene (5.7–5.5 Ma ago)—up to −300 m, and the Early Pleistocene (0.84–0.85 Ma ago)—up to −200 m (Cassian-Turkian regression).

Following this regressive phase, the epoch of equatorial transgression (Figure 1) was succeeded by the epoch of polar transgression, driven by long-term variations in the Earth's rotational form and velocity. The 100,000-year cycle of Earth's orbital eccentricity [45] is a known period during which Earth's orbit changes from nearly circular to slightly elliptical. It has a significant effect on the climate, even though the change in total solar radiation is slight, as epochs of continental glaciation alternated with interglacial periods.

Of the three Late Cenozoic hydrospheric events discussed above, the Akchagylian basin stands out as the most unusual in terms of paleogeography and sedimentation-biotic characteristics (Figures 2 and 3). The paleogeographic map of ancient anthropological sites presented in Figure 2, was compiled through a careful analysis of numerous sources (after Eppelbaum and Katz [1], with supplements). The geodynamic map (Figure 3) displays the main tectonic units and land–sea boundaries during the Akchagylian (Eopleistocene) transgression, overlaid on a satellite-derived gravity map (transformed after polynomial approximation; the map was first calculated in [34]). Our study area lies within the key geodynamic feature of the region—the Mesozoic Terrane Belt—which indicates its tectonic complexity.

3.2. Geodynamic, Paleomagnetic, Structural, and Event Stratigraphy Analysis for the Most Ancient Anthropological Sites in the Levantine Corridor

The ages of the anthropological sites were established using a combination of stratigraphic, radiometric, paleomagnetic, anthropological, and paleogeographic methods, allowing for the estimation of geological sections. Among these, the most critical factors are the land–sea ratio (as inferred from transgressions and regressions) and the stages of climate change. To address the former, we applied the method of hydrospheric disturbances [10], based on measurements of sea terrace levels and river incision amplitudes (Figure 4), which is most effective in relatively stable continental platform regions.

Tectonic–paleomagnetic mapping, essential for understanding the extensive Late Cenozoic deposits that contain numerous ancient hominin sites, requires a detailed analysis of tectonic, geodynamic, paleomagnetic, and other geological events. This analysis underpins both the mapping and the study of ancient hominin abiotic habitats, as well as the estimation of site ages. To achieve this, we examined the general chronostratigraphic framework and correlated the heterogeneous components of Late Cenozoic events with paleomagnetic stratigraphy for the Levant and Paratethys basins.

We expanded the traditional criteria and methods for correlation by incorporating elements of event and cyclic stratigraphy, along with criteria for paleogeographic and tectonic–geodynamic assessment of sequences containing ancient hominin sites. These approaches accounted for the conditions under which preceding and subsequent deposits formed, as well as for stratigraphic discontinuities. We provided a regional justification for the chronostratigraphic nomenclature of the Mediterranean and Paratethys basins, while local magnetostratigraphic divisions were employed to define the stages. This approach is crucial for paleomagnetic stratigraphy, relying on the well-studied paleopedological framework and sea-level fluctuation benchmarks measured in relatively stable areas of

continental platforms. The unification of the tiered scale is crucial, considering the planetary hydrospheric disturbances employed to establish it. These perturbations in the practice of archaeology were considered only on the marine coasts.

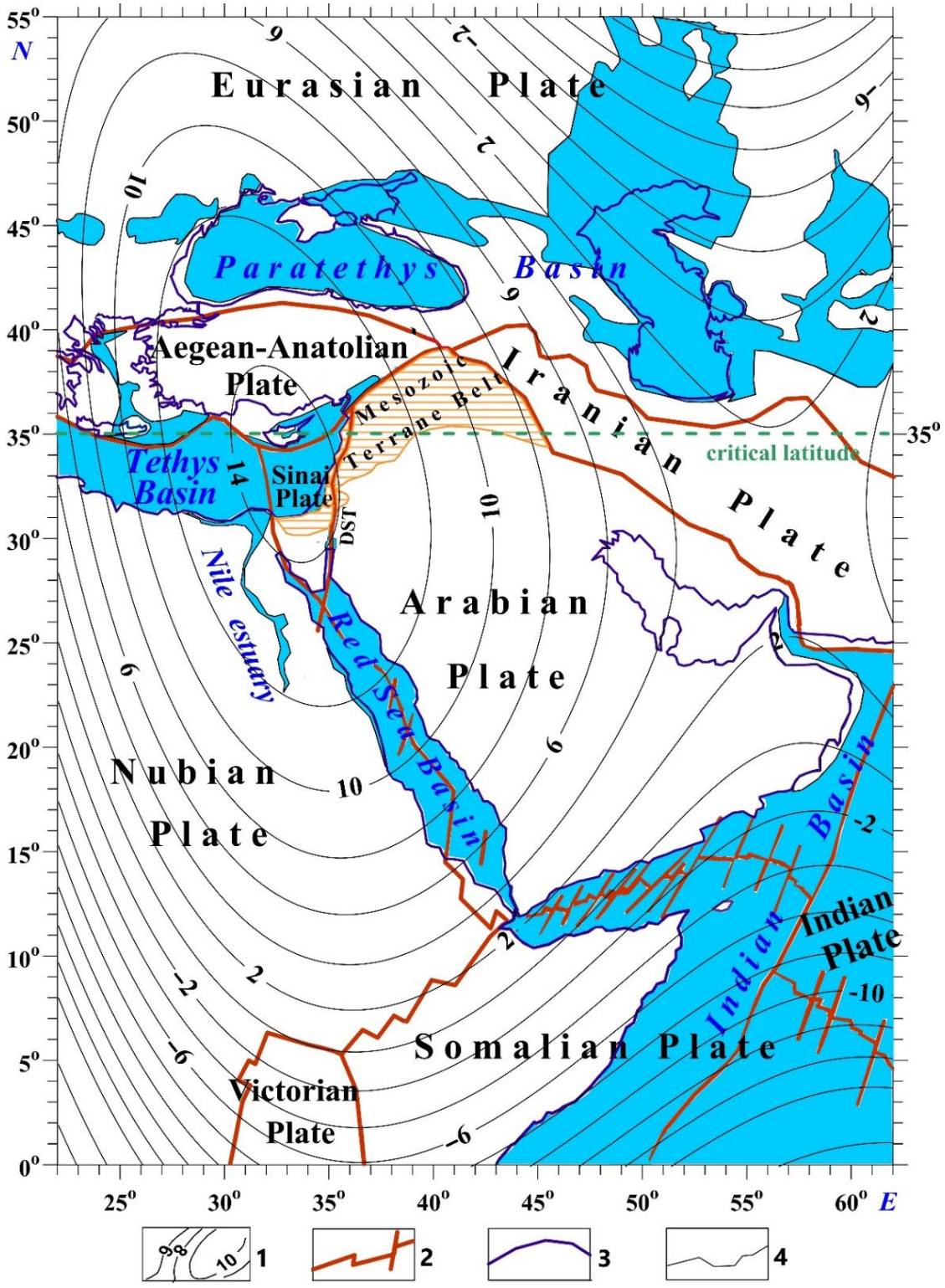


Figure 3. Geodynamic map of the Eurasian–Arabian–Nubian region with the central tectonic units and the land–sea boundaries in the period of the Akchagylian (Eopleistocene) transgression (geophysical and geomorphological components are revised and supplemented after [34] and [10], respectively). (1) isolines of the residual satellite-derived gravity field, (2) interplate faults, (3) present-day land–sea boundaries, (4) land–sea boundaries during the Eopleistocene (Akchagylian–Gelasian) transgression.

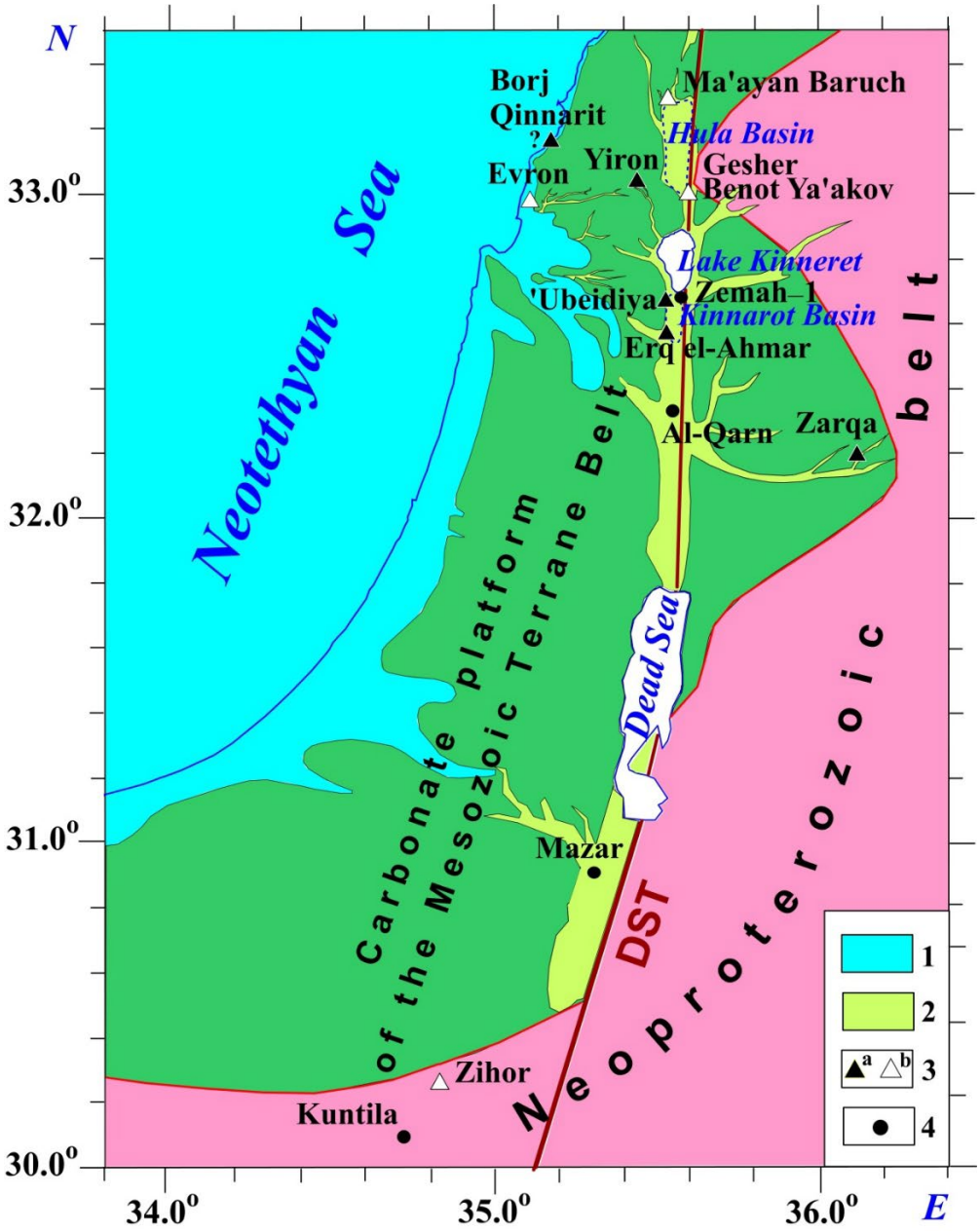


Figure 4. A simplified tectonic-paleogeographic map of the Levantine region for the Gelasian-Akchagylian time of the maximal flooding (revised and supplemented after [1]). (1) areas covered by the Gelasian Sea of Neotethys, (2) areas of the development of alluvial and lacustrine facies of the Gelasian stage, (3) location of the archaeological sites of the ancient hominins considered in the presented study (3a denotes sites from the Akchagylian (Piacenzian-Gelasian) transgression, and 3b—sites from the Absheronian (Calabrian) regression), (4) location of geological sections Kuntila and Mazar (southern Israel), and Zemah-1 borehole (northern Israel) significant for the radiometric, stratigraphic, and paleomagnetic correlation. DST, Dead Sea Transform. The symbol '?' indicates the insufficient knowledge of the geological and archaeological data.

Meanwhile, these factors play a central role in landscape and climate evolution, as fluctuations in the final water-body levels drive the development of extensive ecosystems inhabited by ancient hominins. Consequently, it is valuable to incorporate ecostratigraphic and climatostratigraphic correlation criteria into archaeological stratigraphy, while accounting for the alternation of humid and arid periods (pluvial and dry epochs). In this context, studies of the hydrogeological cycles that regulate hominin development are crucial [77] and warrant dedicated, detailed investigation.

The characteristics of Upper Cenozoic sections and site distributions vary across the Eastern Mediterranean. To address this, tectonic–paleogeographic typification was applied, distinguishing the coastal plain into (1) the Dead Sea Transform (DST) zone of troughs and uplifts and (2) the uplifted plateau of the Neoproterozoic Sinai massif. These regions differ markedly in seismotectonic, landscape-structural, and facies–paleogeographic features, reflecting their relatively younger development compared to the igneous and metamorphic Precambrian Sinai belt. The principal anthropological sites—including the primary site of 'Ubeidiya and key surrounding sites such as Gesher Benot Yakov, Evron, Yiron, Erq el-Ahmar, Zarqa, and Zihor (Figure 4)—are concentrated within these two areas.

The carbonate platform of the Eastern Mediterranean coastal plain (Figure 4) is tectonically subsided [29] and forms part of the modern Levant shelf, and contains predominantly marine sediments, with minor contributions from the Neogene volcanic traps.

In contrast, the Dead Sea Transform (DST) basins contain a diverse range of volcanic and sedimentary deposits of varying ages, including freshwater and brackish lacustrine carbonate–terrigenous strata, as well as alluvial soil sequences associated with river terraces. These regions encompass multiple facies types of sedimentary complexes and terrestrial volcanic rocks, integrated into a unified scheme in Figure 5.

The multi-layered structure of the 'Ubeidiya site indicates prolonged exploitation, suggesting it served as a stable source of freshwater, abundant hunting opportunities, and numerous potentially edible plants [16,24]. Event-stratigraphic and rhythm-stratigraphic analyses reveal that the 'Ubeidiya and Erq el-Ahmar formations exhibit no significant stratigraphic break, forming a continuous sequence of lacustrine–alluvial cycles within the Gauss and Matuyama Chrons [1]. Analogous sequences to these formations have been documented in the Al Qarn section of the Jordan Valley [61] (Figure 4).

Gastropod assemblages from this section [38] demonstrate continuity between the 'Ubeidiya and Erq el-Ahmar formations, indicating that they belong to the same paleogeographic–sedimentological cycle and that significant breaks in earlier sections are unlikely. The facies complexes are summarized in Figure 5, with corresponding symbols to the right of the columns. The columns also indicate the paleomagnetic polarity of the deposits or igneous formations, where present, and the completeness of the sections, which accounts for the size of stratigraphic breaks. The comprehensive paleomagnetic–geological–archaeological correlation enables us, for the first time, to join the mosaic picture of different anthropological sites in the Levant Corridor (and near it) into a single ensemble (Figure 5). This completeness assessment is a crucial component of the event-stratigraphy procedure, which we regard as essential for evaluating the temporal relationships among carefully studied archaeological sites.

Figure 5 shows the horizons containing artifacts alongside the radiometric ages of igneous (right columns) and sedimentary rocks (left columns). Igneous equivalents of the Zanclean period (5.3–3.6 Ma), represented by the Cover Basalt Formation [54,78], are most extensively developed in the Eastern Mediterranean. In the Kinneret–Kinnarot troughs, the thickness of these traps reaches 706 m in the Zemah-1 borehole [59]. This is evidence of the highest level of magmatic activity in the region under study, which undoubtedly influenced the development of ecosystems and the evolution of the ancient hominins. The onset of the Piacenzian stage marks the beginning of the Akchagylian hydrospheric maximum, evidenced by the development of the Erq el-Ahmar lacustrine-alluvial formation within the DST basins (Figure 4). This formation, resting atop the Cover Basalts, predominantly exhibits normal magnetization [25], consistent with the Gaussian Chron [62]. During the subsequent phase of the Akchagylian hydrospheric maximum, the western plateaus were inundated by a sea approximately 200 m above the present level, leading to the extensive formation of the Pleshet marine deposits across Israel's Mediterranean coastal plain [10].

In the Evron section, these marine deposits underlie continental layers containing artifacts and vertebrate remains [13].

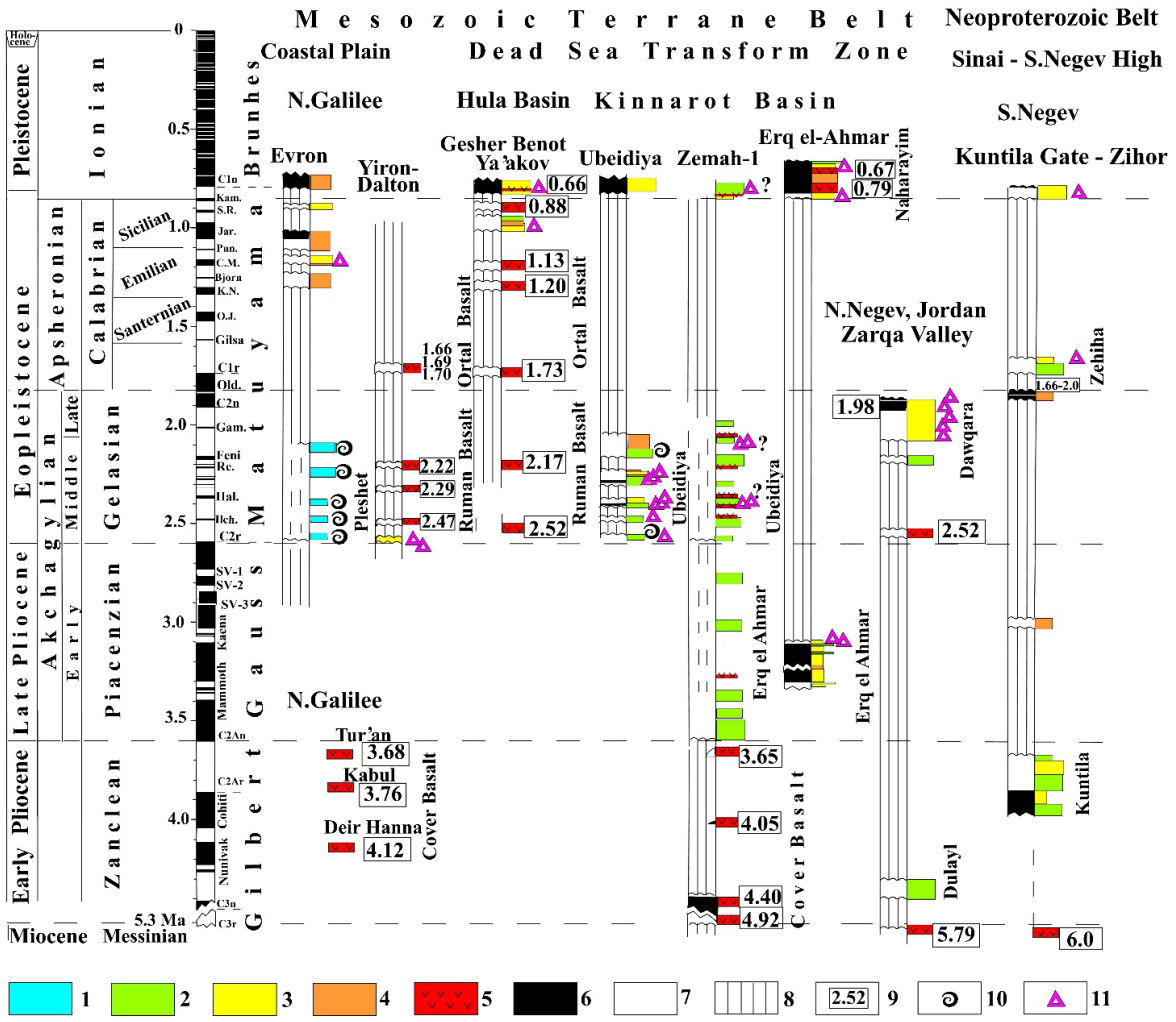


Figure 5. Combined structural, paleomagnetic, and event-stratigraphic chart of ancient hominin sites in the northern Levant (revised and supplemented after [42]). Facies (1–3): (1) marine, (2) lake-swamp, (3) fluvial, (4) soils, (5) basic traps, paleomagnetic polarities (6–7): (6) normal, (7) reversal, (8) gaps, (9) radiometric dating, (10) rests of the marine benthic fauna, (11) discovered artifacts. Paleomagnetic subchrons: Kam., Kamikatsura, S.R., Santa Roza, Jar., Jaramillo, Pun., Punaruu, C.M., Cobb Mt., K.N., Kvemo-Natanebi, O.J., Ontong Java, Old, Olduvai, Gam., Gamarri, Re., Reunion, Hal., Halawa, Ilch., Ilchembet (?), SV(1–3), Searles Valley (1–3).

The paleomagnetic intervals were compiled following the studies of [7,13,17,19,26,31–33,49,61–63,79,80]. The radiometric data were compiled using the studies of [19,27,30,49,59,77,78,81–84]. The marine paleontological remains were compiled based on [36,50]. The artifacts were generalized after [12,16,17,19,20,41,77,84].

In constructing the chart, data from individual archaeological sites, geological sections, and boreholes were employed: Evron [1,13,23,81,85], Yiron [11], Gesher Benot Ya'akov [14,30,50,81]; 'Ubeidiya [12,16,17,21,24,36,49]; Erq el-Ahmar [41,49,61,78]; Kuntila Gate—Zihor [50,63,84]; Zarqa Valley [19], northern Galilee [1,60,82], Zemah-1 well [50,59,86,87].

The palinspastic reconstruction of the period between 3.6 and 2.0 Ma in the Hula, Sea of Galilee, and Kinnarot basins, along with the surrounding uplifts of the Dead Sea Transform (DST), provides insights into the tectonic and magmatic evolution of the 'Ubeidiya anthropological site (see its location in Figure 2) [42].

3.3. Structural-Geomorphological Reconstructions for Northern Israel

The first structural–geomorphological map of Mt. Carmel and its adjacent areas in Galilee (Figure 6) revealed that the tectonic uplift of this mountain in the Miocene-Pliocene period created an island composed of Cretaceous and partly Paleogene carbonate rocks. At the same time, the Galilee area was lowered and almost entirely covered by the Miocene-Pliocene Sea. Based on the analysis of the ages and hypsometry, two terraces are distinguished: low, up to +(100–110) m elevated, and high, up to +200 m elevated (Figure 6).

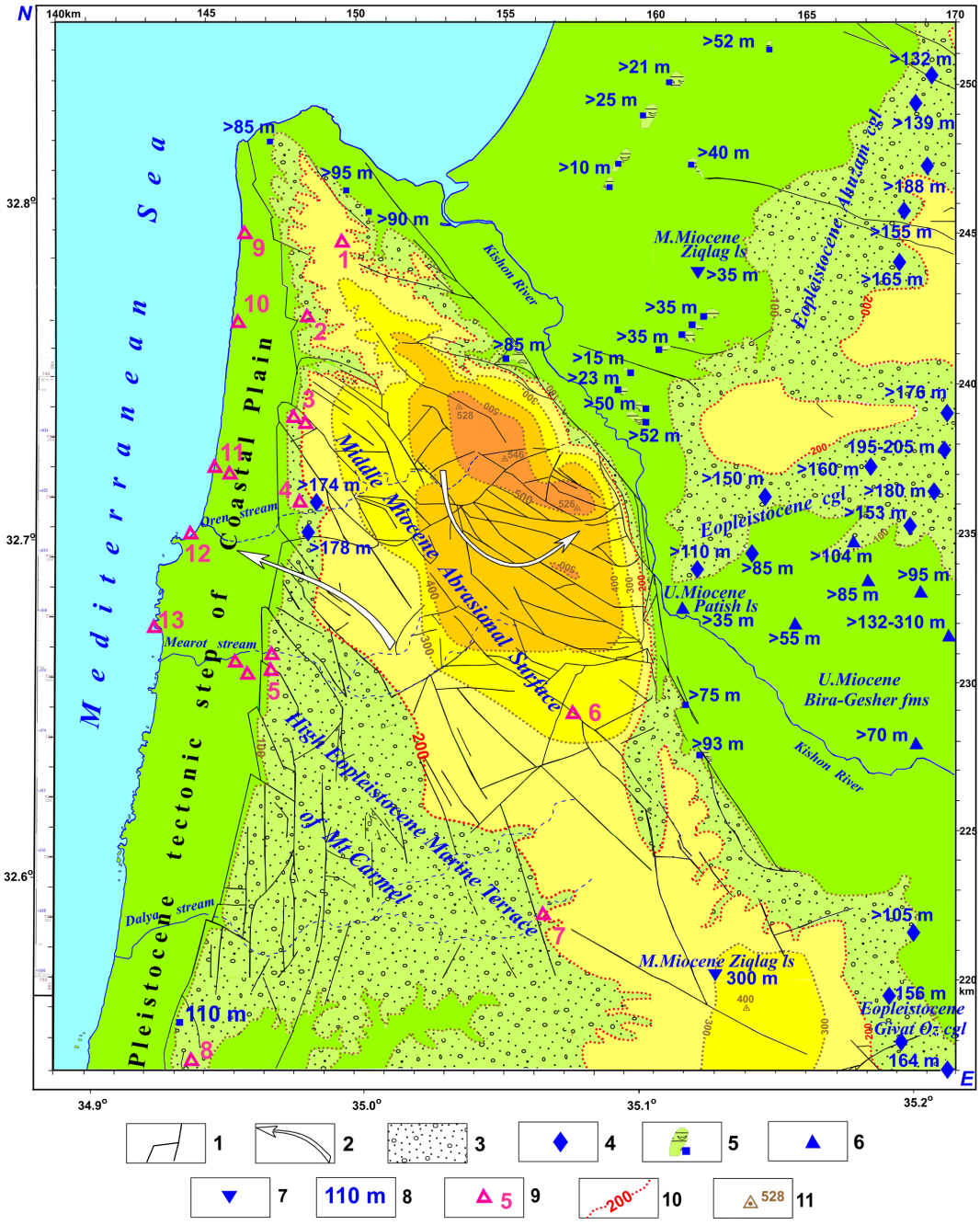


Figure 6. Structural–geomorphological map of the Mt. Carmel area (northern Israel) with the location of ancient archaeological caves (the structural-morphological constructions after [1], with modifications). The following primary works were used in the construction of this map: [15,22,55–58,60,88,89]. (1) faults, (2) counterclockwise rotation of tectonic blocks, (3) high-level Pliocene marine terrace, (4) points with the Pliocene abrasion conglomerates, (5) Pliocene marine sediments of the Pleshet Formation, (6) Late Miocene marine sediments of Bira and Patish Formations, (7) Middle Miocene marine sediments of Ziqlag

Formation, (8) most high level of the marine Pliocene transgression (boundary indicating position of the Miocene islands within the Pliocene marine environments), (9) (large red digits) ancient cave locations relating to different clusters (1–8): 1—Geula cave, 2—Tirat Carmel cave, 2—Mislia and Sfonit caves, 4—Nahal Oren cave, 5—Mearot caves: Nahal Mearot, Es Schul, Tabun, and El Wad, 6—Raqefet cave, 7—Dalya cave, 8—Kebara cave, fishing camps (9–13): 9—Kfar Samir, 10—Kfar Galim, 11—Megadim and Tel Hreiz, 12—Atlit-Yam, 13—Neve-Yam), (10) modern hypsometric data of the Miocene-Pliocene sediments, (11) highest hypsometric points of the tectonically uplifted Miocene marine terraces.

Justification of their stratigraphic sequence, age, conditions of formation, and relationship with the continental Calabrian, its artifacts, and the remains of large-mammal fauna became possible thanks to the study of the unique section in the Evron quarry and its environs (Figure 7). This area in northern Israel (coordinates: 32°59′17.39″ N, 35°06′0.60″ E—see Figure 2) has been studied by numerous experts: geologists, paleontologists, archaeologists, petrographers, and paleomagnetologists (see, for instance, the references in the captions for Figure 7). There are no analogs of such a section in the world, since the combination of the Gelasian marine formations underlain by the trap complex, overlain by continental formations bearing artifacts and remains of large mammals, is an object of study of supreme importance.

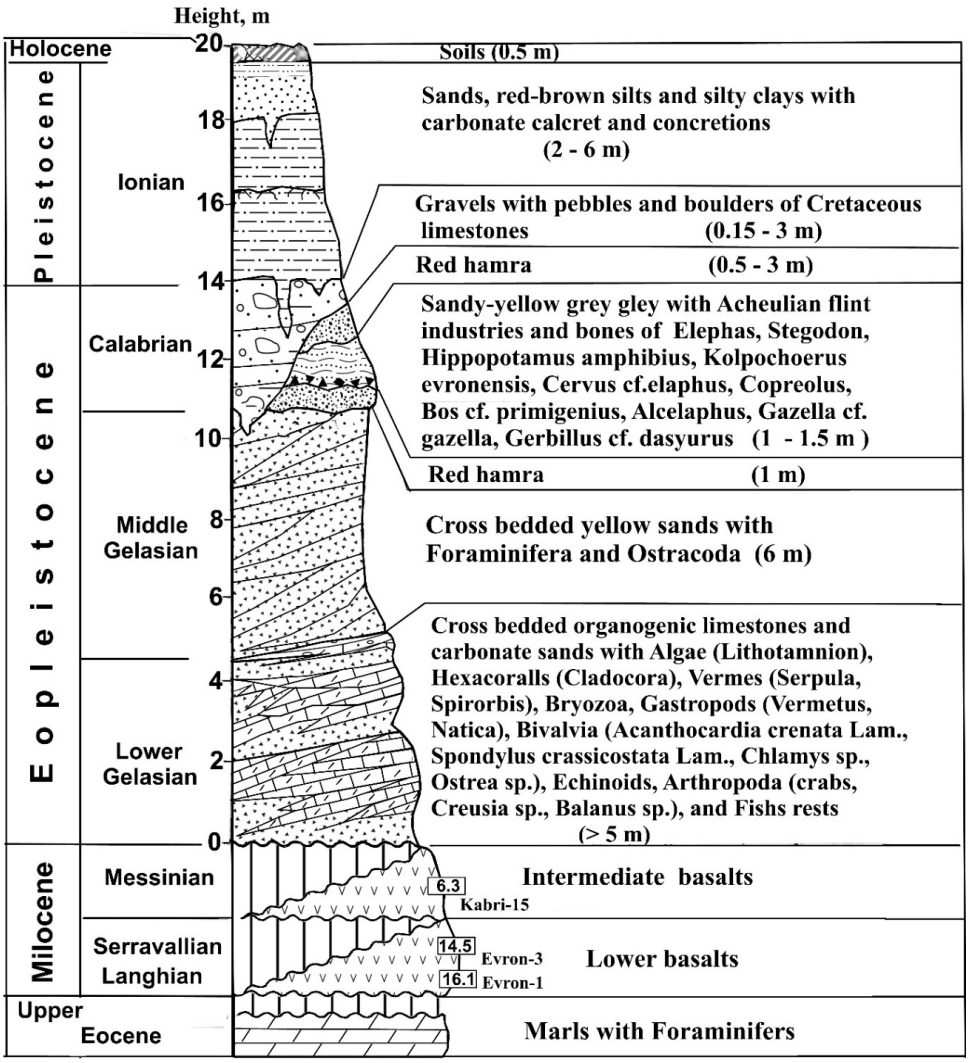


Figure 7. The Upper Cenozoic sediments and traps stratigraphic sequence of the Evron quarry area in northern Galilee (northern Israel) (modified after [51]). This section is based on the authors' personal studies and utilization of the following main works: [1,13,35,39,80,90,91].

The study of anthropological sites involves various methods, including stratigraphic, radiometric, paleomagnetic, anthropological, and paleogeographic techniques, which help estimate geological sections. Among these methods, understanding the land–sea ratio—through the analysis of transgressions and regressions—and examining the stages of climate change are particularly important. To address the first issue, we employed the method of hydrospheric disturbances [10], which involves measuring sea terrace levels and the amplitude of river erosion (Figure 6). This method yields the best results in relatively stable areas of continental platforms.

3.4. Tectonic-Structural and Geophysical Constructions for Central Israel

The significant influence of the Akchagylian (Piacenzian-Gelasian) hydrospheric maximum on the evolution and migration of ancient peoples from Africa to Eurasia is reflected in processes along the coast of the Eastern Mediterranean [51]. According to the tectonic-paleogeographic data (Figures 1–4), during the event under consideration, the western part of the high-carbonate plateau of the Mesozoic Terrane Belt (MTB) was flooded by the sea. In the eastern trough of this plateau, in the DST zone, there was a chain of lake–alluvial basins, along the shores of which are located the ancient hominid sites dating about 2.0–3.0 Ma—'Ubeidiya [16], Yiron [11], Erq el Ahmar [61], and Zarqa [19] (see Figure 2). This pluvial basin was undoubtedly connected with the high-amplitude Gelasian transgressive marine basin—Pleshet formation (Figures 4 and 6). An analog of such a connection between the DST and Eastern Mediterranean basins manifested itself in the previous epoch of more intense transgression of the early Messinian, when thick deposits of depression salts were formed in the pull-apart basins of the DST, and carbonate rock strata were formed on the uplifts aged about 6.0–7.0 Ma [50,51].

Thus, during the considered stage of the hydrospheric maximum of the Akchagylian-Gelasian, the dispersal of early hominids occurred under optimal conditions. Like other landscapes of Africa, Asia Minor, and Transcaucasia, the Levantine Corridor was located on the eastern edge of the carbonate plateau, far from the Mediterranean coastline. This factor may partly explain the comparatively low rate of evolutionary transformations of ancient hominins during the Pliocene hydrosphere maximum in the zone of relatively uniform ecosystems along the migration route from Africa to Asia. To substantiate this position, we employed a comparative analysis, expanding the time frame and examining the later stages of the Levantine Corridor's development. For this purpose, numerous data were used to construct the geological–geophysical maps and profiles presented in Figures 8–10.

The developed geomorphological map (Figure 8) indicates that, during the Eopleistocene (the period of the Absheronian-Calabrian hydrosphere minimum), almost the entire space of the carbonate plateau of the MTB rose above the Eastern Mediterranean Basin. In the Pleistocene, with the onset of glacioeustatic movements (approximately 800–850 Kyr ago), the formation of transgressive-regressive complexes began, caused by the Milankovitch [45] rhythm (approximately 100 Kyr), associated with the eccentricity of the Earth's orbit. Processes of a similar scale had not occurred in the late Cenozoic before. They have also significantly influenced nature and the rate of change in landscapes and ecosystems. It is pretty evident that such a radical geodynamic, climatic, paleogeographic, and ecosystemic restructuring of the planet caused a more intensive growth of the ecumene and led to a sharp increase in the evolutionary diversity of hominids at the beginning of the Pleistocene epoch, even though vast areas of the continents of Eurasia, North America and the south of Gondwana were covered by the continental glaciation.

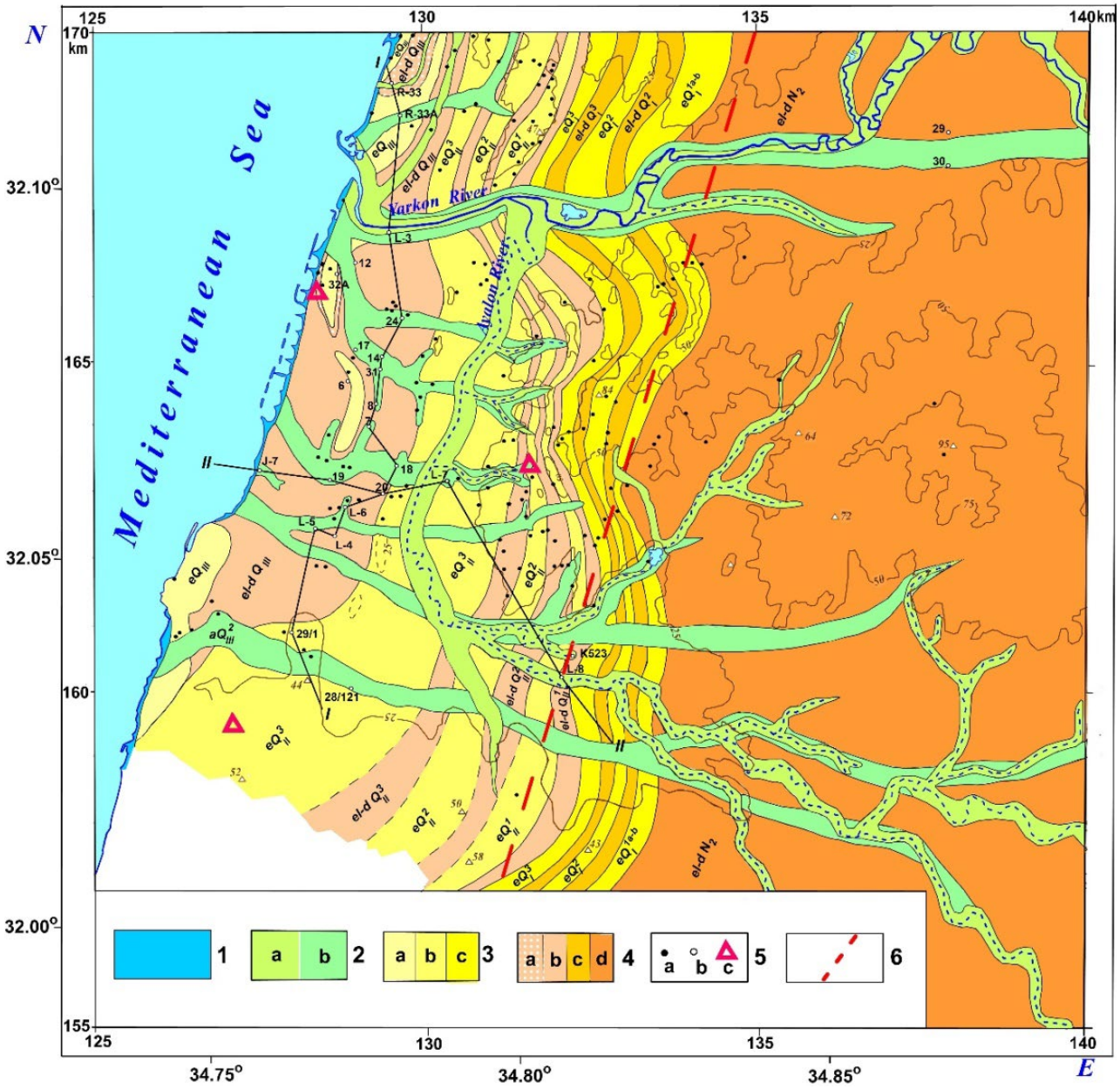


Figure 8. Geomorphological map of the Pleistocene ridges and the Late Pliocene plateau of the Levantine Corridor in the Gush Dan coastal plain (central Israel). The locations of the archaeological sites are based on those reported in [15] and by the authors of this paper. (1) coastal–marine Holocene formations within natural coastal and technogenic complexes, 2 (a, b) alluvial landforms: (2a) Holocene, (2b) Middle–Upper Pleistocene, 3 (a–c) aeolian landforms of the coastal dune ridge complex: (3a) Upper Pleistocene, (3b) Middle Pleistocene, (3c) Lower Pleistocene, 4 (a–d) eluvial–diluvial landforms of the period of eccentric glacial regressive phases of the Pleistocene and the Late Pliocene Calabrian hydrospheric minimum [1,51]: (4a) pre-Holocene, (4b) Middle–Upper Pleistocene, (4c) Lower Pleistocene, (4d) Upper Pliocene, 5 (a, b, c) reference section locations: (5a) outcrops, (5b) boreholes, (c) archaeological sites, (6) tectonic fault line of the western coastal block of the Gush Dan coastal plain (according to the geophysical and geomorphological data).

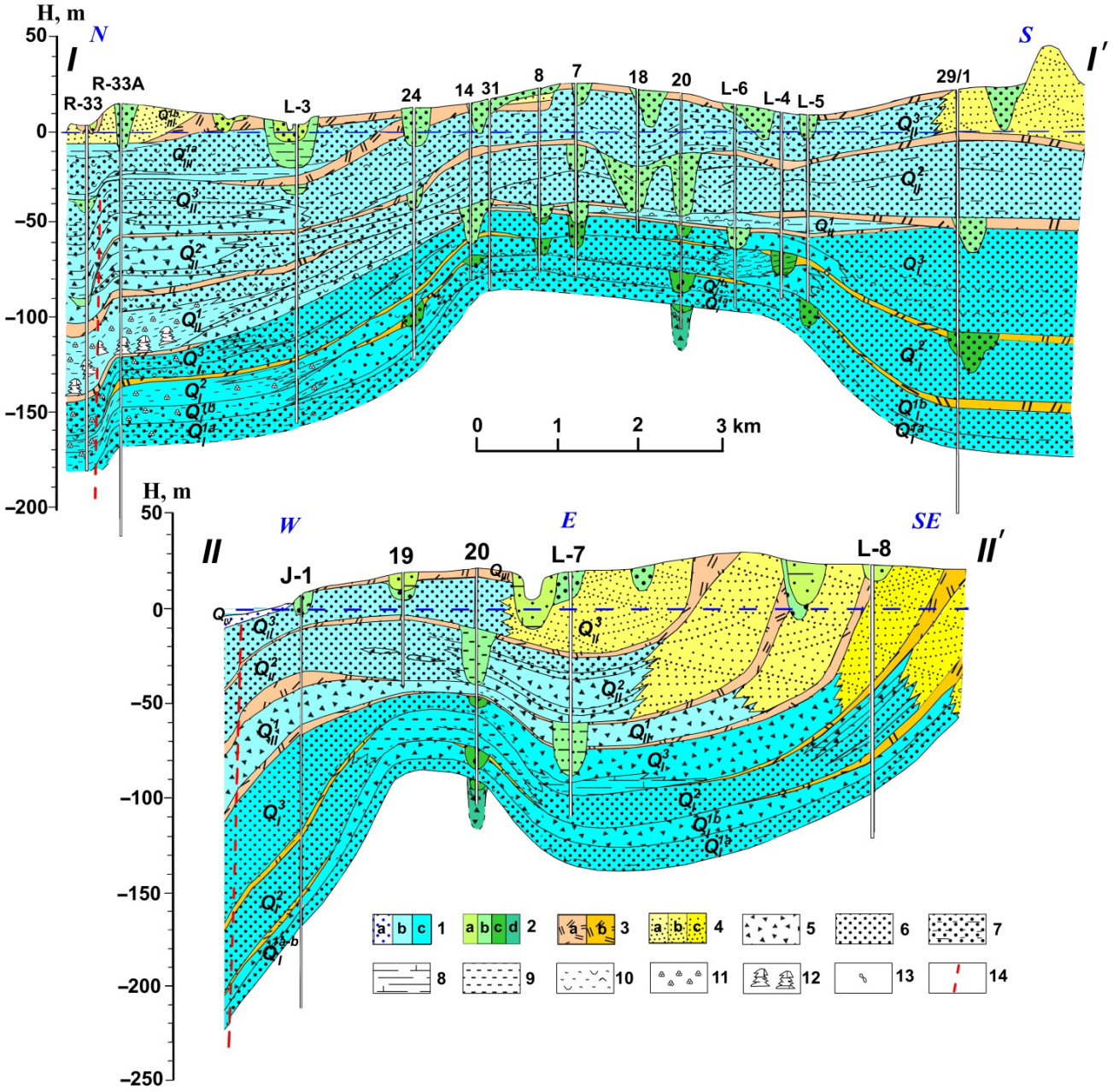


Figure 9. The Quaternary facies-stratigraphic profiles (I-I and II-II) of the coastal part of the Levantine Corridor in the Gush Dan area (central Israel). (1a–c): marine sediments: (1a) Holocene submarine and coastal terraces, (1b) tectonically uplifted Middle-Upper Pleistocene marine terraces, (1c) Lower Pleistocene uplifted marine terraces, (2a–d): alluvial series of fluvial incision: (2a) Holocene, (2b) Middle–Upper Pleistocene, (2c) Lower Pleistocene, (2d) initial stage of the Pleistocene incision, (3a–b): Upper-Middle Pleistocene, (3b) Lower Pleistocene, (4a–c) tectonically uplifted ridges of the aeolian coastal series: (4a) Upper Pleistocene, (4b) Middle Pleistocene, (4c) Lower Pleistocene, (5) coarse-grained sedimentary series, (6) sandy sedimentary series, (7) sandy-silty formations, (8) silty marine facies, (9) clayey marine and lagoonal facies, (10) marine shell horizons, (11) remains of the large foraminifera, (12) organogenic structures of the marine immersion zone, (13) remains of the mammal bones, (14) zones of tectonic ruptures.

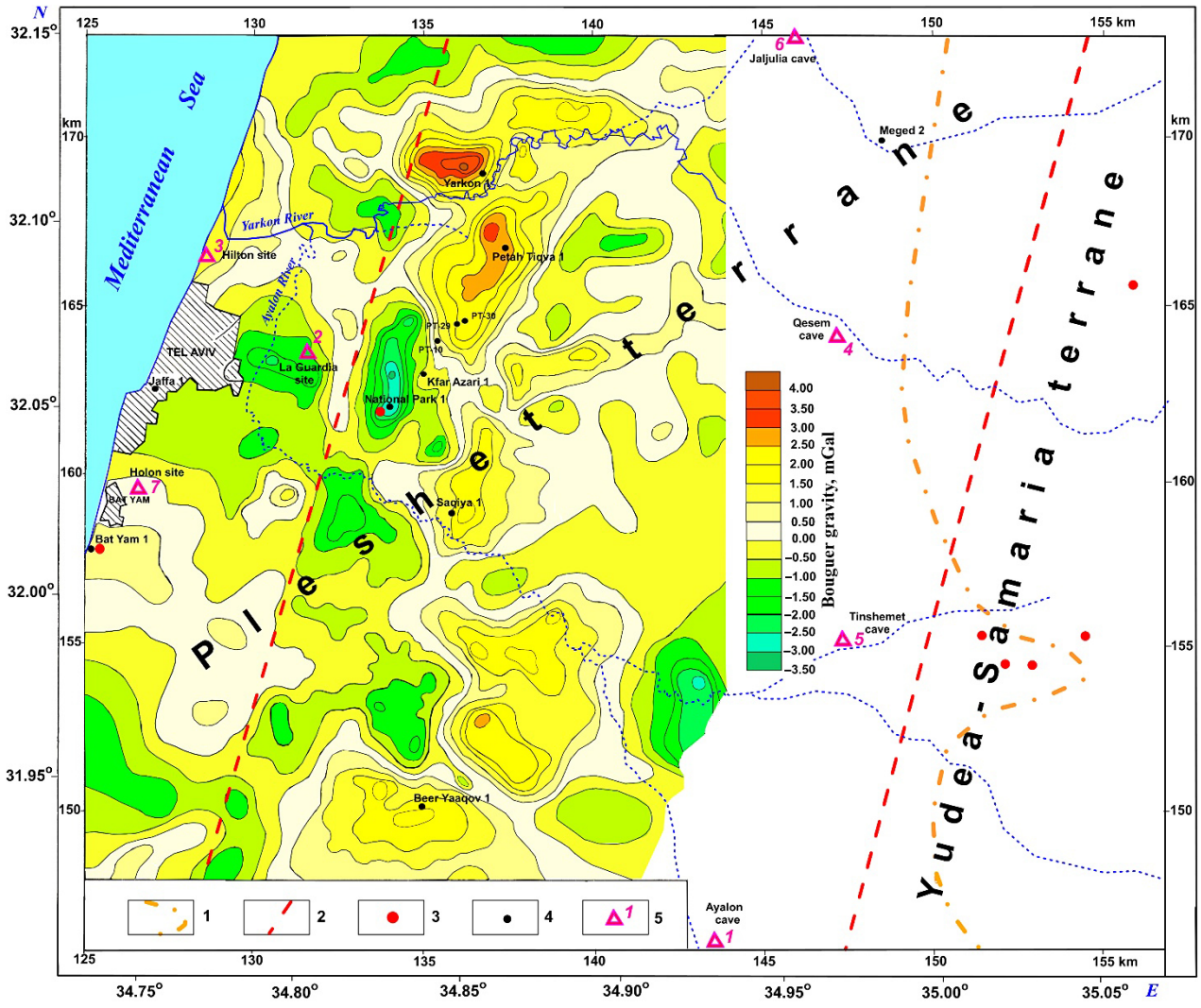


Figure 10. The residual Bouguer gravity map of the Gush Dan region (central Israel) (around the mid-1960s; the initial data are from the personal archive of Prof. A. Ginzburg (Tel Aviv University); revised and supplemented by the authors of this paper), with the main tectonic elements. (1) eastern limit of the subsurface Neogene, (2) faults, (3) Neogene magmatism in the outcrops and boreholes, (4) main boreholes, (5) archaeological site locations (after [15,18,22,23], and the authors of the paper): *1*—Ayalon cave, *2*—La Guardia Neolithic fishing site, *3*—Hilton site, *4*—Qesem cave, *5*—Tinshemet cave, *6*—Jaljulia cave, *7*—Holon site.

Lines I–I and II–II are, respectively, the longitudinal and transverse profiles in the zone of Pleistocene deposit development in the western coastal plain of the Gush Dan area. These profiles reflect the characteristic relief of the Levantine Corridor during the epoch of glacial hydroeustasy and isostatic adjustment of unstable terrane massifs in the Eastern Mediterranean Coastal Plain.

When subdividing the well sections into profiles, we used classical age-analysis methods for the Pleistocene formations. Glacial (regressive) and interglacial (transgressive) complexes are clearly distinguished from each other. For the coastal plain of Israel, we rely on the data of Gvirtzman et al. [47], who identified the "Kurkar group"—a complex of dune and marine formations from the interglacial era—and a complex of soil-alluvial red bed formations ("hamra") from the epoch of glacial regressions. The difference in the rhythmic sequence of Pleistocene sedimentary formations (see Figures 11 and 12) is characterized by complex facies, as reflected in the legend to Figure 9.

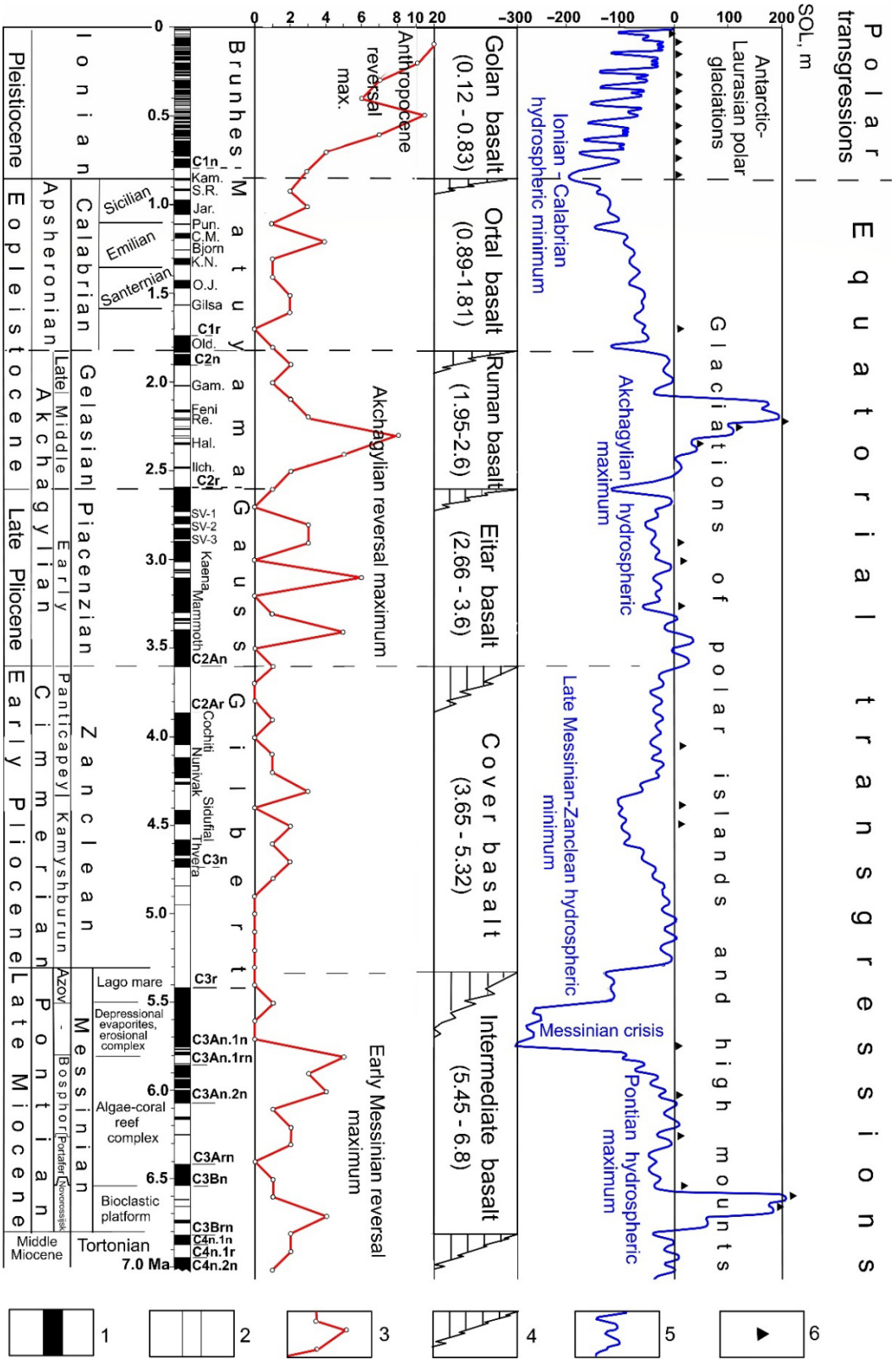


Figure 11. Distribution scheme of paleomagnetic, tectonothermal, hydrospheric, glacial, and rotational rhythms in the late Cenozoic sections of the Mediterranean Sea—Paratethys region. (1) magnetic field normal polarity, (2) magnetic field reverse polarity, (3) curve of changes in paleomagnetic reversals over 100 Kyr, (4) stratigraphic break between the cycles of late Cenozoic trap complexes of the Dead Sea Transform (Galilee—Golan Plateau) region, (5) cycles of oscillations of the hydrosphere curve of the Neotethys—Paratethys basins, (6) glacial stages of the continental and mountain glaciations.

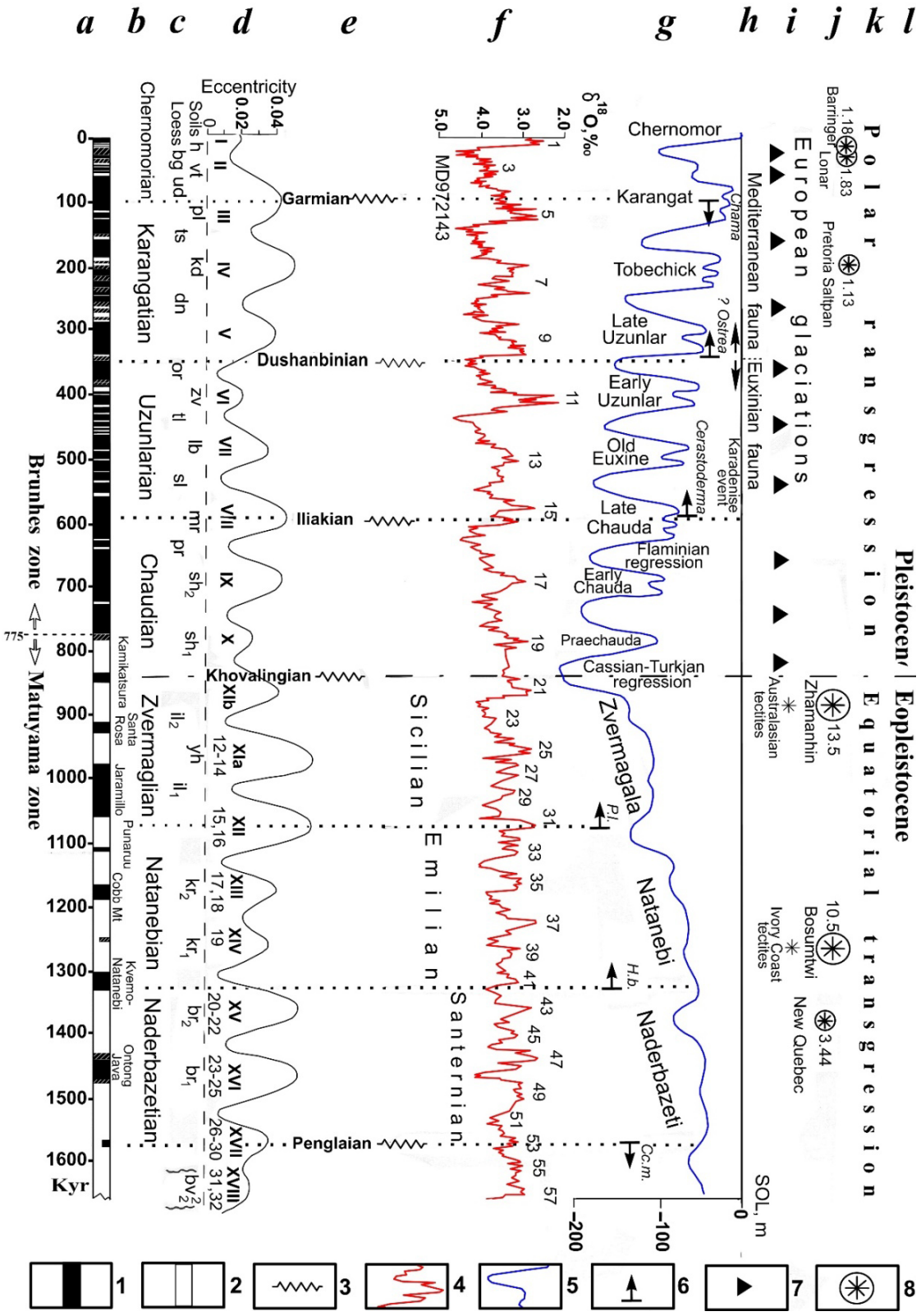


Figure 12. Event-stratigraphic-paleomagnetic scale of the final part of the Cenozoic of the Mediterranean—Paratethys region. (1) magnetic field of normal polarity, (2) magnetic field of reverse polarity, (3) tectonic phases, (4) cycles of oscillations of the isotope-oxygen curve, (5) cycles of oscillations of the hydrosphere curve, (6) phases of development of supporting faunal benchmarks, (7) phases of the continental glaciations, (8) impact craters with the diameter indications (in km). (a) Paleomagnetic-geochronological scale (in Kyr), (b) ecostratigraphic rhythms in 250 Kyr, (c) soil-loess

(paleopedological) scale of the reference paleomagnetic sections of the extraglacial zone of the Southern Ukraine [26], (d) rhythms of the Earth's orbit eccentricity in sections of the soil-loess series of Central Asia [92], (e) tectonic phases of 250 Kyr from the same sections, (f) isotope-oxygen curve from the oceanic borehole MD 972,143 [28], (g) curve of the hydrospheric disturbances along the sections of the Black Sea basin, (h) Karadeniz horizon with the fauna of the Mediterranean mollusks in the Black Sea basin, (i) cycles of the continental glaciations of the European platform, (j) impact basins and tektite horizons [48], (k) stages of the Earth's rotational rhythms, (l) subdivisions of the standard stratigraphic scale.

On the other hand, in addition to the differentiated movements, the profiles also reflect a consistent increase in the level of the hydrosphere from the Early to the Late Pleistocene, although these data require a more careful analysis. The longitudinal profile I-I in the Gush Dan (Figure 9) shows a consistent overlap in conditions of a relatively stable tectonic block near the Mediterranean coast, characterized by the cyclically constructed Pleistocene terrace complexes, from the lower to the upper. Their hypsometric levels roughly correspond to the curve of hydrospheric fluctuations of the Pleistocene basins shown in Figure 1.

However, the transverse profile II-II in the Gush Dan (Figure 9) shows a structural paradox: the more ancient terrace complexes (judging by their eastern boundaries, remote from the modern coast) occupy a larger area than the younger Pleistocene formations, which seems to indicate not a transgressive, but a regressive sequence of occurrence from the ancient horizons to the young ones. This paradox arises because the eastern blocks of the MTB underwent significant uplift during the Pleistocene. In contrast, the western blocks sank toward the coastline and further into the Mediterranean Sea. This effect is visible in both the transverse profile II-II and the residual gravity-tectonic map of Gush Dan (Figure 10). The map presented in Figure 10 is exceptional since the gravity data were observed in the non-developed Gush Dan area; now the repetition of such a survey is complicated by many buildings constructed since the 1960s (which implies the need to introduce a vast number of gravity corrections with the blurred density). The abovementioned facts allow us to assess the nature of the formation processes of the coastal Levantine Corridor during the Pleistocene, particularly in the development of the Pleshet and Judea-Samaria terranes.

As can be seen on profiles I-I and II-II, the marine Pleistocene terraces and the associated aeolian dune ridges ('Kurkar' group), underlain by regressive, red-colored formations of the glacial epochs ('hamra'), are cut by sharply unconformable river valleys. They are composed of heterogeneous alluvial complexes. One of these incisions, clearly visible on profile II-II (Figure 9), is associated with the La Guardia archaeological site (eastern Tel Aviv). On this site, the authors identified remains of a heterogeneous Pleistocene-Holocene ancient flint industry featuring numerous microliths.

Here, three unstable systems of tectonic steps parallel to each other have been identified using tectonic-geophysical, paleogeographic, and radiochronometric data. They differ hypsometrically and in gravity anomaly distribution, and they are marked no less paleogeographically. The first step, located on the western boundary of the Judea-Samaria terrane plateau, is marked by the eastern boundary of the Neogene marine basins [53] and the development of folded structures within the thickness of the Upper Cretaceous limestones and dolomites. The second step encompasses the most significant part of the Pleshet terrane, with the eastern ends of the Pleistocene terraces marking its western boundary. The step of the west, which is the smallest in area and width, is limited by both the modern coastline and the Holocene marine terraces, as well as tectonic faults recorded at the coastal ends of the longitudinal and transverse profiles (Figure 9). A key indicator of geodynamic instability in the formation of the Levantine Corridor along the coastal carbonate platform is the occurrence of Late Miocene–Early Pliocene traps, dated to

approximately 3.5–6.8 Ma [50], observed in both outcrops and borehole sections near the major fault zones (Figure 10).

4. Discussion

Thus, the presented materials demonstrate the contrast between the colossal transgression of the Akchagylian–Gelasian age preceding continental glaciation and the regression and landscape change during the Pleistocene age of glacial-eustatic movements, coinciding with the period of polar transgression. At this time, the coastal part of the high carbonate plateau of the Mesozoic Terrane Belt (MTB) collapsed, and on its border with the Eastern Mediterranean basin, the Levantine Corridor was formed, represented by a variety of landscapes from coastal–marine to soil–continental, river, and eolian facies (Figures 8 and 9). During the Akchagylian–Gelasian period, ancient hominins migrated from Africa along the DST trough and inhabited the lake-river basin, which was partly connected to the Gelasian Sea basin in the Lower Galilee [10]. Then, in the Pleistocene, new hominids mastered a narrow coastal migration zone—the Levantine Corridor, where frequent landscape changes occurred under conditions of contrasting climatic transformations between the glacial and interglacial epochs, associated with the vast Eurasian lithospheric plate.

An analysis of the geodynamic changes in the Earth's mantle and core during the Late Cenozoic is essential for understanding the peculiarities of ecosystem development and the dispersal routes of ancient people from Africa to Eurasia. In the presented analysis of transformations in the deep and surface shells, only the most essential elements are considered: paleomagnetic, tectonic-thermal, hydrospheric, glacial, and rotational (Figure 11). They clearly indicate the fundamental connection between the evolution and migration of hominids and the deep and surface geophysical processes of a cyclic nature.

An analysis of magnetic field reversal frequency clearly shows alternating maxima and minima, which are undoubtedly associated with transformations in the Earth's core shells [43,44]. Tectonic–thermal processes recorded in the change of the DST trap complexes [27,29] indicate a clear correlation not only with the paleomagnetic, but also with the hydrospheric cycles, especially with the Pleistocene (Ionian) and Akchagylian (Gelasian-Piacenzian).

Since for the first time in the practice of paleogeographic analysis of the conditions of ancient people settlement, a detailed cartographic analysis of ecosystems with sites of both ancient (Late Pliocene-Eopleistocene) and later (Pleistocene) hominins of the Eastern Mediterranean and the Levantine Corridor was carried out, a natural need arose for a geological-geophysical substantiation of the stage differences of the Early and Late Levantine Corridor. For this purpose, we used a more diverse and extensive range of studies in the field of historical planetology and event stratigraphy than in the analysis of early (Figures 4, 5 and 11)—late Pliocene–Eopleistocene (Akchagylian–Apsheronian) hominin sites (Figure 12). First, when analyzing the paleomagnetic scale, it was established that the glacioeustatic epoch of the Pleistocene, where the hydrospheric disturbances generally correspond to the rhythm of the Earth's orbit eccentricity of about 100 Kyr, is almost entirely located within the boundaries of zone 1n (Brunhes) and the uppermost part of zone 1r (Upper Matuyama).

Thus, the regime of predominantly normal polarity of the Earth's magnetic field during the Pleistocene glacial epoch serves as a fundamental planetary geophysical marker of this period. The cycles of Earth's orbital eccentricity [93] have been thoroughly studied in the soil–loess sequences of the Tajik Depression, particularly to the east of the Caspian Sea [92]. In the Mediterranean–Paratethys region under investigation, the orbital eccentricity rhythm [93] and the paleomagnetic scale [26] are corroborated by paleopedological reference studies, clearly demonstrating the predominance of glacial loess layers within the

Pleistocene section. Soil layers comprise nearly the entire paleopedological complexes of the Eopleistocene.

According to the sections of the tectonically active Tajik depression, rhythms of 250 Kyr [92] with clearly defined tectonic phases and erosional unconformities [94] are well recorded in the Pleistocene. Based on tectonic–sedimentary and paleomagnetic data, these same rhythms were revealed in the Eopleistocene of the Black Sea region [79,95], and with a high degree of probability, can be correlated with the marine terrace sections of the Eopleistocene in the Mediterranean. In addition, a specific correlation is observed between the hydrospheric disturbances (Figure 12g) and the registered significant impact events (Figure 12j). The latter fact requires separate and thorough analysis.

The use of the isotope–oxygen curve from the section of the deep-sea basin of the World Ocean (well MD 972,143) [28] reveals a classic pattern of fluctuations in the water background, reflecting the intensity of the glacial processes. In the period of the polar transgression and widespread development of continental glaciations, according to the isotope-oxygen curve, a clear correspondence is manifested between the fluctuations in the water background and the rhythms of the Earth's orbit eccentricity (100 Kyr), and in the Eopleistocene these fluctuations are close to the rhythm of the obliquity of the ecliptic (obliquity) of about 40 Kyr, which many researchers noted. The connection of the Mediterranean waters with the Paratethys waters through the Marmara Sea system manifested itself 250 Kyr after the beginning of the Pleistocene, at the end of the Chaudinian Age, when the larvae of the *Cerastoderma* mollusks, whose shells had not reached the size of the adult stage, penetrated the desalinated basin of the Black Sea. After the same period of 250 Kyr, at the beginning of the late Uzunlar Age [46], benthic ecosystems with a more complex array of marine mollusks from Mediterranean waters (*Ostreidae* and others) began to develop.

In the period of the maximum salinity development of the Black Sea waters, approximately 30 ppm in the Karangatian Age, mollusks living in normal salinity conditions began to form (*Chama* sp., *Acanthocardia tuberculata*, and others). The observed Karadeniz faunal migration event, clearly linked to a 250 Kyr rhythm (Figure 12), suggests a connection with the plate geodynamic processes at the Central Gondwana–Eurasia boundary, whose activity was governed by the circular motions of a lithosphere influenced by deep mantle structure movement [34].

A comparative event-stratigraphic analysis of the late Cenozoic, along with the attached cartographic material on the terranes of the coastal plain of the late Levantine Corridor (Figures 8 and 10), showed the identity of the classic marine terrace complexes of the Black Sea and more extensive marine terraces developed in the coastal zone of the Eastern Mediterranean. Unlike the uplifting terranes of Crimea and the Caucasus, where Pleistocene terraces form, the marine terrace complexes of the Levantine Corridor are associated with the subsidence system of the Mesozoic Terrane Belt at the contact with the oceanic basin of the Levantine Basin (Figure 3). This is one of the most mobile geodynamic zones of the Earth, corresponding to the apical part of the regional structure of the deep mantle.

The glacial cycles clearly illustrate the connection between Earth's figure transformations and Earth's rotation speed. During the Miocene-Eocene, only sporadic glacial processes developed, associated with glaciations in the uplifts of the island lands of polar countries and the mountain ranges of middle latitudes. Moreover, true continental glaciations of planetary scale developed only during the period of polar transgressions, beginning approximately 850 Kyr ago.

The planetary transformations of Earth's shells undoubtedly affected the ecosystems along the route of hominin dispersal from Africa to Eurasia, first in the geodynamically unstable Eastern Mediterranean zone, including the Levantine migration corridor.

At the turn of the Pleistocene and Holocene—in the Neolithic age—cave-type sites were replaced by land-based coastal fishing camps [22] in the Carmel coastal region (Figure 6) and river settlements in the Gush Dan area (Figures 8 and 10), featuring a complex of diverse microliths. The diversity of artifacts in the Pleistocene of the Levantine Corridor, compared to the more ancient artifacts of the Lower Galilee and Jordan in the DST depression located to the east, well illustrates the more frequent hominin evolutionary transformations during their movement from Africa to Asia after the maximum flooding in the Neotethys and Paratethys basins during the Akchagylian–Gelasian age. Since these basins were located near the critical parallel of 35° [34], block tectonic movements had a significantly differentiated character. This affected both the plate geodynamics (Figure 3) and the character of the formation of the Levantine Corridor (Figures 4, 8 and 10), as indicated by geomorphological, stratigraphic, radiochronometric, and geophysical data.

It is important to note that during the Gelasian–Akchagylian hydrospheric maximum, the uplifted edge of the carbonate platform of the MTB was covered by a high transgression from the Eastern Mediterranean, and the submerged part of this high plateau—the primary Levantine Corridor—was in the DST depression zone between the Sinai and Arabian lithospheric plates. Furthermore, during the transitional period of the post-Akchagylian (Calabrian–Apsheronian) regression, the Levantine Corridor lay within the same DST area. However, at this time, neotectonic subsidence occurred in the carbonate plateau's marginal region, leading to the formation of the initial western branch of the Levantine Corridor. Finally, during the glacioeustatic Pleistocene transgressive-regressive epoch, the pluvial regime characteristic of the Akchagylian maximum was resumed, and under these conditions, two branches of the Levantine migration corridor of ancient hominins were formed: the western one, in the Coastal Plain of the neotectonically lowered edge of the carbonate platform, and the eastern one, in the DST depression. This exceptional combination of pluvial conditions and varied environmental settings—from continental uplands to the seacoast—along the extended dual route of the Levantine migration corridor likely played a decisive role in influencing both the pace of evolution and the patterns of human dispersal from Africa to Eurasia.

It should be noted that, according to our comprehensive paleomagnetic, tectonic, and structural analysis [51], the age of the famous Ubeidiya site (see its location in Figure 2) can be 1.8–2.6 Ma (Figure 5). This period corresponds to the Akchagylian–Gelasian hydrospheric maximum (Figure 11).

Therefore, the formation of the younger Levantine Corridor in the Pleistocene Coastal Plain well shades both epochs. The problem under study is well complemented by the gravity-tectonic map (Figure 10), which shows the geodynamic instability of the plateau carbonate platform covered by the Akchagylian–Gelasian Sea, with the subsequent subsidence of the plateau, the formation of the Levantine Corridor, and the advancement of new hominins along it, experiencing the more frequent evolution.

5. Conclusions

From the research presented, the following conclusions can be drawn:

(1) The significant Akchagylian hydrospheric maximum (up to +200 m; during ~2.4–1.9 Ma) has limited the early hominin dispersal from Africa to Eurasia.

(2) The large-scale dispersal of ancient people resumed after the end of the Akchagylian hydrospheric event on ~1.9 Ma.

(3) During the Akchagylian-Gelasian hydrospheric maximum, the uplifted edge of the carbonate platform of the MTB was covered by a high transgression from the Eastern Mediterranean, and the submerged part of this high plateau—the primary Levantine Corridor—was in the DST depression zone.

(4) In the transitional period of the post-Akchagylian (Calabrian–Apsheronian) regression, some neotectonic subsidence of the marginal part of the carbonate plateau occurred with the formation of the initial western branch of the Levantine Corridor.

(5) Through the glacioeustatic Pleistocene transgressive–regressive epoch, the pluvial regime characteristic of the Akchagylian maximum was resumed. Under these conditions, two branches of the Levantine migration corridor for ancient hominids were formed: the western branch in the Coastal Plain, adjacent to the neotectonically lowered edge of the carbonate platform, and the eastern branch in the DST depression.

(6) The presented analysis may be used as a basis for further investigations of the geodynamic influences on the ancient hominin dispersal.

Author Contributions: L.V.E. and Y.I.K.—equivalent contributions to all sections of this paper. All authors have read and agreed to the published version of the manuscript.

Funding: This research received no external funding.

Data Availability Statement: The original contributions presented in this study are included in the article. Further inquiries can be directed to the corresponding author(s).

Conflicts of Interest: The authors declare no conflicts of interest.

References

1. Eppelbaum, L.; Katz, Y. Combined Zonation of the African-Levantine-Caucasian Areal of Ancient Hominin: Review and Integrated Analysis of Paleogeographical, Stratigraphic and Geophysical-Geodynamical Data. *Geosciences* **2022**, *12*, 21. [CrossRef]
2. Bennison, G.M.; Wright, A.E. *The Geological History of the British Isles*; Edward Arnold: London, UK, 1969; 143p.
3. Chumakov, I.S. Pliocene and Pleistocene deposits of the Nile Valley in Nubia and Upper Egypt. In *Transactions of the Geological Institute of RAS*; Nauka: Moscow, Russia, 1967; Volume 170, 115p. (In Russian)
4. Camps, M.; Chauhan, P. (Eds.) *Sourcebook of Paleolithic Transitions*; Springer: Dordrecht, The Netherlands, 2009; 574p.
5. Clauzon, G.; Suc, J.-P.; Dumurdžanov, N.; Melinte-Dobrinescu, M.C.; Zagorchev, I. The Pliocene Gilbert-type fan delta of Draĉevo (Skopje area, Republic of Macedonia): Paleogeographic inference. *Geol. Maced.* **2008**, *2*, 21–28.
6. Richards, K.; van Baak, C.G.C.; Athersuch, J.; Hoyle, T.M.; Stoica, M.; William, E.N.; Austin, W.E.H.; Cage, A.G.; Wonders, A.A.H.; Marreti, F.; et al. Palynology and micropalaeontology of the Pliocene—Pleistocene transition in outcrop from the western Caspian Sea, Azerbaijan: Potential links with the Mediterranean, Black Sea and the Arctic Ocean? *Palaeogeogr. Palaeoclimat. Palaeoecol.* **2018**, *511*, 119–143. [CrossRef]
7. Krijgsman, W.; Tesakov, A.; Yanina, T.; Lazarev, S.; Danukalova, G.; Van Baak, C.G.; Agustí, J.; Alçiçek, M.C.; Aliyeva, E.; Bista, D.; et al. Quaternary time scales for the Pontocaspian domain: Interbasinal connectivity and faunal evolution. *Earth-Sci. Rev.* **2019**, *188*, 1–40. [CrossRef]
8. Ben-Avraham, Z.; Lazar, M.; Schattner, U.; Marco, S. The Dead Sea Fault and its Effect on Civilization. In *Perspectives in Modern Seismology*; Lecture Notes in Earth Sciences, Wenzel, F., Eds.; Springer: Berlin/Heidelberg, Germany, 2005; Volume 105, pp. 147–170. Available online: https://link.springer.com/chapter/10.1007/978-3-540-31563-6_9 (accessed on 12 August 2025).
9. Horowitz, A. The Quaternary stratigraphy and paleogeography of Israel. *Paléorient* **1977**, *3*, 47–100. [CrossRef]
10. Eppelbaum, L.; Katz, Y. Akchagylian Hydrospheric Phenomenon in Aspects of Deep Geodynamics. *Stratigr. Sediment. Oil-Gas Basins* **2021**, *2*, 8–26.
11. Ronen, A. The Yiron-gravel lithic assemblage artifacts older than 2.4 My in Israel. *Archologisches Korresp.* **1991**, *21*, 159–164.
12. Bar-Yosef, O.; Goren-Inbar, N. The Lithic Assemblages of 'Ubeidiya: A Lower Paleolithic Site in the Jordan Valley. *Oedem* **1993**, *45*, 1–266. Available online: http://www.jstor.org/stable/43587057 (accessed on 12 August 2025).
13. Tchernov, E.; Horwitz, L.K.; Ronen, A.; Lister, A. The Faunal Remains from Evron Quarry in Relation to Other Lower Paleolithic Hominid Sites in the Southern Levant. *Quat. Res.* **1994**, *42*, 328–339. [CrossRef]
14. Goren-Inbar, N.; Feibel, C.S.; Verosub, K.L.; Melamed, Y.; Kislev, M.E.; Tchernov, E.; Saragusti, I. Pleistocene Milestones on the Out-of-Africa Corridor at Gesher Benot Ya'aqov, Israel. *Science* **2000**, *289*, 944–947. [CrossRef]

15. Gopher, A.; Ayalon, A.; Bar-Matthews, M.; Barkai, R.; Frumkin, A.; Karkanas, P.; Shahack-Gross, R. The chronology of the late Lower Paleolithic in the Levant based on U-TH ages of speleothems from Qesem cave, Israel. *Quat. Geochronol.* **2010**, *5*, 644–656. [CrossRef]
16. Bar-Yosef, O.; Belmaker, M. Early and Middle Pleistocene faunal and hominins dispersals through Southwestern Asia. *Quat. Sci. Rev.* **2011**, *30*, 1281–1295. [CrossRef]
17. Bar-Yosef, O.; Belmaker, M. Ubeidiya. In *Quaternary of the Levant, Part III: Archaeology of Human Evolution*; Enzel, Y., Bar-Yosef, Y., Eds.; Cambridge University Press: Cambridge, UK, 2017; pp. 179–186.
18. Hershkovitz, I.; Weber, G.W.; Fornai, C.; Gopher, A.; Barkai, R.; Slon, V.; Quam, R.; Gabet, Y.; Sarig, R. New Middle Pleistocene dental remains from Qesem Cave (Israel). *Quat. Int.* **2016**, *398*, 148–158. [CrossRef]
19. Scardia, G.; Parenti, F.; Miggins, D.P.; Gerdes, A.; Araujo, A.G.M.; Neves, W.A. Chronologic constraints on hominin dispersal outside Africa since 2.48 Ma from the Zarqa Valley, Jordan. *Quat. Sci. Rev.* **2019**, *219*, 1–19. [CrossRef]
20. Herzlinger, G.; Brenet, M.; Varanda, A.; Deschamps, M.; Goren-Inbar, N. Revisiting the Acheulian Large Cutting Tools of Ubeidiya, Israel. *J. Paleolit. Archaeol.* **2021**, *4*, 31. [CrossRef]
21. Barash, A.; Belmaker, M.; Bastir, M.; Soudack, M.; Oaley, D.H.D.; Woodward, H.; Prendergast, A.; Barzilai, O.; Been, E. The earliest Pleistocene record of a largest Pleistocene from the Levant supports two out-of-Africa dispersal events. *Sci. Rep.* **2022**, *12*, 1721. [CrossRef]
22. Galili, E.; Rosen, B.; Gopher, A.; Kolska-Horwitz, L. The Emergence and Dispersion of the Eastern Mediterranean Fishing Village: Evidence from Submerged Neolithic Settlements off the Carmel Coast, Israel. *J. Mediterr. Archaeol.* **2002**, *15*, 167–198. [CrossRef]
23. Shemer, M.; Greenbaum, N.; Taha, N.; Brailovsky-Rokser, L.; Ebert, Y.; Shaar, R.; Falgueres, C.; Voinchet, P.; Porat, N.; Faerstein, G.; et al. Late Acheulian Jaljulia—Early human occupations in the paleolandscape of the central coastal plain of Israel. *PLoS ONE* **2022**, *17*, e0267672. [CrossRef]
24. Mallol, C. What's in a beach? Soil micromorphology of sediments from the Lower Paleolithic site of 'Ubeidiya, Israel. *J. Hum. Evol.* **2006**, *51*, 185–206. [CrossRef]
25. Davis, M.; Matmon, A.; Fink, D.; Ron, H.; Niedermann, S. Dating Pliocene lacustrine sediments in the central Jordan Valley, Israel—Implications for cosmogenic burial dating. *Earth Planet. Sci. Lett.* **2011**, *305*, 317–327. [CrossRef]
26. Tretyak, A.N.; Vigilyanskaya, L.I.; Makarenko, V.N.; Dudkin, V.P. *Fine Structure of the Geomagnetic Field in the Late Cenozoic*; Naukova Dumka: Kiev, Ukraine, 1989; pp. 155–165. (In Russian)
27. Mor, D.A. A time-table for the Levant Volcanic Province, according to K-Ar dating in the Golan Heights. *Isr. J. Afr. Earth Sci.* **1993**, *16*, 223–234. [CrossRef]
28. Horng, C.S.; Roberts, A.P.; Liang, W.T. A 2.14-Myr astronomically tuned record of relative geomagnetic paleointensity from the western Philippine Sea. *J. Geophys. Res.* **2003**, *108*, 2059. [CrossRef]
29. Eppelbaum, L.V.; Katz, Y.I. Paleomagnetic Mapping in Various Areas of the Easternmost Mediterranean Based on an Integrated Geological Geophysical Analysis. In *New Developments in Paleomagnetism Research, Ser: Earth Sciences in the 21st Century*; Eppelbaum, L., Ed.; Nova Science Publisher: Hauppauge, NY, USA, 2015; pp. 15–52.
30. Probokormi, M.S.; Urban, B.; Mischke, S.; Mienis, H.K.; Melamed, J.; Dupont-Nivet, G.; Jourdan, F.; Goren-Inbar, N. Evidence for climatic changes around the Matuyama-Brunhes Boundary (MBB) inferred from a multi-proxy paleoenvironmental study of the GBY #2 core, Jordan River Valley, Israel. *Palaeogeogr. Palaeoclimatol. Palaeoecol.* **2018**, *489*, 166–185. [CrossRef]
31. Behar, N.; Shaar, R.; Tauxe, L.; Asefaw, H.; Ebert, Y.; Heimann, A.; Koppers, A.A.P.; Ron, H. Paleomagnetism and paleosecular variations from the Plio-Pleistocene Golan Heights volcanic plateau, Israel. *Geochem. Geophys. Geosyst.* **2019**, *20*, 4319–4335. [CrossRef]
32. Cohen, K.M.; Gibbard, P.L. Global chronostratigraphical correlation table for the last 2.7 million years, version 2019 QI-500. *Quat. Int.* **2019**, *500*, 20–31. [CrossRef]
33. Channell, J.E.T.; Singer, B.S.; Jicha, B.R. Timing of Quaternary geomagnetic reversals and excursions in volcanic and sedimentary archives. *Quat. Sci. Rev.* **2020**, *228*, 106114. [CrossRef]
34. Eppelbaum, L.V.; Ben-Avraham, Z.; Katz, Y.; Cloetingh, S.; Kaban, M. Giant quasi-ring mantle structure in the African-Arabian junction: Results derived from the geological-geophysical data integration. *Geotectonics* **2021**, *55*, 67–93. [CrossRef]
35. Issar, A.; Kafri, U. The Discovery of a Pleistocene Mammalian Fauna and artefacts at Evron, Western Galilee. *Isr. J. Earth Sci.* **1969**, *18*, 147.
36. Almogi-Labin, A.; Siman-Tov, R.; Rosenfeld, A.; Debard, E. Occurrences and distribution of the foraminifer Ammonia beccari tepida (Cushman) in water bodies, recent and quaternary of the Dead Sea Rift, Israel. *Mar. Micropaleontol.* **1995**, *26*, 153–159. [CrossRef]
37. Semaw, S.; Simpson, S.W.; Quade, J.; Renne, P.R.; Butler, R.F.; McIntosh, W.C.; Levin, N.; Dominguez-Rodrigo, M.; Rogers, M.J. Early Pliocene hominids from Gona, Ethiopia. *Nature* **2005**, *433*, 301–305. [CrossRef]
38. Bandel, K.; Sivan, N.; Heller, J. Melanopsis from Al-Qarn, Jordan Valley (Gastropoda: Gerithioidea). *Palaontol. Z.* **2007**, *81*, 304–315. [CrossRef]

39. Belmaker, M. Early Pleistocene Faunal Connections between Africa and Eurasia. In *An Ecological Perspective. Out of Africa I: The First Hominin Colonization of Eurasia, Vertebrate Paleobiology and Paleoanthropology*; Fleagle, J.G., Shea, J., Grine, F., Baden, A., Leakey, R., Eds.; Springer: Dordrecht, The Netherlands, 2010; pp. 183–205. [CrossRef]
40. Naidina, O.D.; Richards, K. The Akchagylian stage (late Pliocene–early Pleistocene) in the North Caspian region: Pollen evidence for vegetation and climate change in the Ural-Emba region. *Quat. Int.* **2020**, *540*, 22–37. [CrossRef]
41. Rabinovich, R.; Herzlinger, G.; Calvo, G.; Rivals, F.; Mischke, S.; Beiner, G. Erq el Ahmar Elephant Site—A mammoth skeleton at a rare and controversial Plio-Pleistocene site along the mammal migration route out of Africa. *Quat. Sci. Rev.* **2019**, *221*, 105885. [CrossRef]
42. Eppelbaum, L.V.; Katz, Y.I. Multidisciplinary Geological-Geophysical Analysis Unmasks Anthropological Site Structure in the Northern Part of the Levantine Corridor. *J. Anthropol. Archaeol. Sci.* **2023**, *8*, 1056–1078. Available online: https://lupinepublishers.com/anthropological-and-archaeological-sciences/fulltext/multidisciplinary-geological-geophysical-analysis-unmasks-anthropological-site-structure-in-the-northern-part-of-the-levantine-corridor.ID.000286.php (accessed on 12 August 2025).
43. Braginsky, S.I.; Meytlis, V.P. Local turbulence in the Earth's core. *Geophys. Astrophys. Fluid Dyn.* **1990**, *55*, 71–87. [CrossRef]
44. Holdenried-Chernoff, D.; Buffett, B.A. Evidence for Turbulent Magnetic Diffusion in Earth's Core. *Geochem. Geophys. Geosyst.* **2002**, *3*, e2022GC010672. [CrossRef]
45. Milankovitsch, M. *Canon of Insolation and the Ice-Age Problem*; Spec. Publication of the Royal Serbian Academy: Belgrade, Serbia, 1941; Volume 132, 634p.
46. Katz, Y.I.; Smyslov, G.A. *New Data on the Stratigraphy and Conditions of Formation of the Pleistocene Deposits of the Kerch Peninsula*; Bull. of Kharkov. University, No. 136. Ser: Geology and Geography, No. 7; Vishcha Shkola: Kharkov, Ukraine, 1976; pp. 13–19. (In Russian)
47. Gvirtzman, G.; Shachnai, E.; Bakar, N.; Bani, S. *Stratigraphy of the Kurkar Group of the Coastal Plain of Israel*; Israel Geological Survey, Current Research: Jerusalem, Israel, 1984; pp. 70–82.
48. Grady, M.M. *Catalogue of Meteorites*, 5th ed.; Cambridge University Press: Cambridge, UK, 2000; 689p.
49. Heimann, A.; Braun, D. Quaternary stratigraphy of the Kinnarot Basin, Dead Sea Transform, northeastern Israel. *Isr. J. Earth Sci.* **2000**, *49*, 31–44. [CrossRef]
50. Hall, J.K.; Krasheninnikov, V.A.; Hirsch, F.; Benjamini, C.; Flexer, A. *Geological Framework of the Levant*; Vol. II: The Levantine Basin and Israel; Historical Productions-Hall: Jerusalem, Israel, 2005; 826p.
51. Eppelbaum, L.V.; Katz, Y.I. African-Levantine Areal of Ancient Hominin Dispersal: A New Look Derived from Comprehensive Geological-Geophysical Integration. In *Emerging Issues in Environment, Geography and Earth Science*; Yousef, A.F., Ed.; BP International: London, UK, 2024; Volume 7, pp. 151–222. [CrossRef]
52. Rubini, M.; Gozzi, A.; Altamura, F.; Spanò, F.; Zaio, P. A rediscovered fossil hominin fragment from Gombore IB, an early Pleistocene site of Melka Kunture (Upper Awash, Ethiopia). *Quat. Int.* **2025**, *729*, 109792. [CrossRef]
53. Sneh, A.; Bartov, Y.; Weissbrod, T.; Rosensaft, M. *Geological Map of Israel, 1:200,000 (4 Sheets)*; Geological Survey of Israel: Jerusalem, Israel, 1998.
54. Weinstein, Y.; Navon, O.; Altherr, R.; Stein, M. The Role of Lithospheric Mantle Heterogeneity in the Generation of PlioPleistocene Alkali Basaltic Suites from NW Harrat Ash Shaam (Israel). *J. Petrol.* **2006**, *87*, 1017–1050. [CrossRef]
55. Segev, A.; Sass, E. *Sheet 3-III, Atlit. Geological Map of Israel, Scale 1:50,000*; Geological Survey of Israel: Jerusalem, Israel, 2010.
56. Karcz, J.; Sneh, A. *Sheet 3-I, Haifa. Geological Map of Israel, Scale 1:50,000*; Geological Survey of Israel: Jerusalem, Israel, 2011.
57. Sass, E.; Dekel, A.; Sneh, A. *Sheet 5-II, Umm el Fahm. Geological Map of Israel, Scale 1:50,000*; Geological Survey of Israel: Jerusalem, Israel, 2013.
58. Sneh, A.; Sass, E.; Bein, A.; Arad, A.; Rosensaft, M. *Sheet 5-I, Hadera. Geological Map of Israel, Scale 1:50,000*; Geological Survey of Israel: Jerusalem, Israel, 2014.
59. Segev, A. *Zemah-1, a Unique Deep Oil Well on the Dead Sea Fault Zone, Northern Israel: A New Stratigraphic Amendment*; Report GSI/21/2017; Geological Survey of Israel: Jerusalem, Israel, 2017; pp. 1–27.
60. Sneh, A. *Sheet 3-IV, Nazerat. Geological Map of Israel, Scale 1:50,000*; Geological Survey of Israel: Jerusalem, Israel, 2018.
61. Braun, D.; Ron, H.; Marco, S. Magnetostratigraphy of the hominid tool-bearing Erk el Ahmar Formation in the northern Dead Sea Rift. *Isr. J. Earth Sci.* **1991**, *40*, 191–197.
62. Cande, S.C.; Kent, D.V. Revisited calibration of the geomagnetic polarity timescale for the Late Cretaceous and Cenozoic. *J. Geophys. Res.* **1995**, *100*, 6093–6095. [CrossRef]
63. Larrasoaña, J.C.; Waldmann, N.; Mischke, S.; Avni, J.; Ginat, H. Magnetostratigraphy and Paleoenvironments of the Kuntila Lake Sediments, Southern Israel: Implications for Late Cenozoic Climate Variability at the Northern Fringe of the Saharo-Arabian Desert Belt. *Front. Earth Sci.* **2020**, *8*, 173. [CrossRef]

64. Plummer, T.W.; Oliver, J.S.; Finestone, E.M.; Ditchfield, P.W.; Bishop, L.C.; Blumenthal, S.A.; Lemorini, C.; Caricola, I.; Bailey, S.E.; Herries, A.I.R.; et al. Expanded geographic distribution and dietary strategies of the earliest Oldowan hominins and Paranthropus. *Nature* **2023**, *379*, 561–566. [CrossRef]
65. Harmand, S.; Lewis, J.E.; Feibel, C.S.; Lepre, C.J.; Prat, S.; Lenoble, A.; Boës, X.; Quinn, R.L.; Brenet, M.; Arroyo, A.; et al. 3.3-million-year-old stone tools from Lomekwi 3, West Turkana, Kenya. *Nature* **2015**, *521*, 310–315. [CrossRef]
66. Grine, F.E.; Leakey, M.G.; Gathago, P.N.; Brown, F.H.; Mongle, C.S.; Yang, D.; Jungers, W.L.; Leakey, L.N. Complete permanent mandibular dentition of early Homo from the upper Burgi Member of the Koobi Fora Formation, Ileret, Kenya. *J. Hum. Evol.* **2019**, *131*, 152–175. [CrossRef]
67. McDougall, I.; Brown, F.H.; Fleagle, J.G. Sapropels and the age of hominins Omo I and II, Kibish, Ethiopia. *J. Hum. Evol.* **2008**, *55*, 409–420. [CrossRef]
68. Johanson, D. The paleoanthropology of Hadar, Ethiopia. *Comptes Rendus Palevol* **2017**, *16*, 140–154. [CrossRef]
69. Alemseged, Z.; Wynn, J.G.; Geraads, D.; Reed, D.; Barr, W.A.; Bobe, R.; McPherron, S.P.; Deino, A.; Alene, M.; Sier, M.J.; et al. Fossils from Mille-Logya, Afar, Ethiopia, elucidate the link between Pliocene environmental changes and Homo origins. *Nat. Commun.* **2020**, *11*, 2480. [CrossRef] [PubMed]
70. Ozherel'yev, D.V.; Trifonov, V.G.; Chekik, H.; Trihunkov, Y.I. New Evidence of the Early Paleolithic in the Mountain Systems of Eastern Anatolia and the Lesser Caucasus. In *The Earliest Occupation of the Caucasian Region*; Lapshin, V.A., Ed.; Transactions of the Institute for the History of Material Culture of the Russian Academy of Sciences: Sankt-Petersburg, Russia, 2020; pp. 99–127. (In Russian)
71. Veliyev, C.C.; Aleskerov, B.D.; Tagiyeva, E.N. The age of the Azykh site and climatic factors of migration to the Caucasus of the most ancient people. Karabakh in the Stone Age. In Proceedings of the International Scientific Conference Dedicated to the 50th Anniversary of the Discovery of the Paleolithic Cave Site of Azykh in Azerbaijan, Baku, Azerbaijan, 3–7 October 2010; pp. 46–62.
72. Belyaeva, E.V. History of Acheulean studies in Armenia and VP Lyubin's contribution. In *The Earliest Occupation of the Caucasian Region*; Lapshin, V.A., Ed.; Transactions of the Institute for the History of Material Culture of Russian Academy of Sciences: St. Petersburg, Russia, 2020; pp. 55–69. (In Russian)
73. Lordkipanidze, D.; Jashashvili, T.; Vekua, A.; de León, M.S.P.; Zollikofer, C.P.E.; Pontzer, H.; Ferring, R.; Oms, O.; Tappen, M.; Bukhsianidze, M.; et al. Postcranial evidence from early Homo from Dmanisi, Georgia. *Nature* **2007**, *449*, 305–310. [CrossRef]
74. Derevianko, A.P.; Anoykin, A.A.; Kazansky, A.Y.; Matasova, G.G. New Data to Justify the Age of Early Paleolithic Artifacts of Rubas-1 Site (Seaside Dagestan). *Hist. Sci. Archaeol.* **2015**, *No. 1*, 78–83. [CrossRef]
75. Amirkhanov, H.A. Paleolithic culture of the Caucasus at the end of the Eopleistocene: Oldovan, Early Acheulean, transitional stage? *Russ. Archaeol.* **2020**, *2*, 7–21. [CrossRef]
76. Schelinsky, B.E. *The Early Acheulean of Western Ciscaucasia*; The Institute of the Material Culture History, Russian Academy of Sciences: Sankt-Petersburg, Russia, 2021; pp. 132–140. (In Russian)
77. Feibel, C.S. Quaternary lake margins of the Levant Rift Valley. In *Human Paleoecology in the Levantine Corridor*; Goren-Inbar, N., Speth, J.D., Eds.; Oxbow Books: Oxford, UK, 2004; pp. 21–36.
78. Eppelbaum, L.; Ben-Avraham, Z.; Katz, Y. Integrated analysis of magnetic, paleomagnetic and K-Ar data in a tectonic complex region: An example from the Sea of Galilee. *Geophys. Res. Lett.* **2004**, *31*, L19602. [CrossRef]
79. Grishanov, A.I.; Eremin, V.N.; Imnadze, Z.A.; Kitovani, T.G.; Kitovani, S.K.; Molostovsky, E.A.; Torozov, R.I. Stratigraphy of the Upper Pliocene and Upper Pleistocene deposits of Guria (Western Georgia) based on paleontological and paleomagnetic data. In *Bulletin of the Committee for the Study of the Quaternary Period*; Nauka: Moscow, Russia, 1983; pp. 18–28. (In Russian)
80. Ron, H.; Porat, N.; Ronen, A.; Tchernov, E.; Horwitz, L.K. Magnetostratigraphy of the Evron Member—Implications for the age of the Middle Acheulian site of Evron Quarry. *J. Hum. Evol.* **2003**, *44*, 633–639. [CrossRef]
81. Heimann, A. The Development of the Dead Sea Rift and Its Margins in Northern Israel During the Pliocene and Pleistocene. Ph.D. Thesis, Hebrew University, Jerusalem, Israel, 1990; pp. 1–114, (In Hebrew, summary in English).
82. Shaliv, G. Stages in the Tectonics and Volcanic History of the Neogene Basalt in the Lower Galilee and the Valleys. Ph.D. Thesis, Hebrew University, Jerusalem, Israel, 1991. (In Hebrew, summary in English).
83. Heimann, A.; Stenitz, G.; Mor, D.; Shaliv, G. The Cover Basalt Formation, its age and its regional and tectonic setting: Implications from K-Ar and 40Ar/39Ar geochronology. *Isr. J. Earth Sci.* **1996**, *45*, 55–71.
84. Ginat, H.; Zilberman, E.; Saragusti, I. Early Pleistocene lake deposits and Lower Paleolithic finds in Nahal (wadi) Zihor, Southern Negev desert, Israel. *Quat. Res.* **2003**, *59*, 445–458. [CrossRef]
85. Shemer, M.; Crouvi, O.; Shaar, R.; Ebert, Y.; Matmon, A.; ASTER Team; Kolska Horwitz, L.; Eisenmann, V.; Enzel, Y.; Barzilai, O. Geochronology, paleogeography, and archaeology of the Acheulian locality of 'Evron Landfill in the western Galilee, Israel. *Quat. Res.* **2018**, *91*, 729–750. [CrossRef]
86. Marcus, E.; Slager, J.; Ben-Zaken, S.; Indik, I.Y. *Zemah-1. Geological Completion Report 84/11*; Oil Exploration Ltd.: Ramat Hasharon, Israel, 1984; 128p.

87. Marcus, E.; Slager, J. The sedimentary-magmatic sequence of the Zemah-1 well (Jordan-Dead Sea rift, Israel) and its emplacement in time and space. *Isr. J. Earth Sci.* **1985**, *34*, 1–10.
88. Galili, E.; Eshed, V.; Rosen, B.; Kislev, M.E.; Simchoni, O.; Hershkovitz, I.; Gopher, A. Evidence for a separated burial ground at the submerged Pottery Neolithic site of Neve-Yam, Israel. *Paleorient* **2009**, *35*, 31–46. [CrossRef]
89. Sneh, A. *Sheet 3-II, Shefar'Am. Geological Map of Israel, Scale 1:50,000*; Geological Survey of Israel: Jerusalem, Israel, 2013.
90. Ronen, A.; Amiel, A. The Evron quarry: A contribution to the Quaternary stratigraphy of the coastal Plain of Israel. *Paléorient* **1974**, *2*, 167–173. [CrossRef]
91. Ilani, S.; Kafri, U.; Harlavan, Y. Miocene volcanism in the Western Galilee coastal plain. *Isr. J. Earth Sci.* **2005**, *54*, 47–53. [CrossRef]
92. Dodonov, A.E. *Anthropogene of Southern Tajikistan*; Nauka: Moscow, Russia, 1986; 165p. (In Russian)
93. Berger, A.; Loutre, M.F. Insolation values for the climate of the last 10 million years. *Quat. Sci. Rev.* **1991**, *10*, 297–317. [CrossRef]
94. Metzger, S.; Gągała, Ł.; Ratschbacher, L.; Lazecký, M.; Maghsoudi, Y.; Schurr, B. Tajik depression and Greater Pamir neotectonics from InSAR rate maps. *J. Geophys. Res. Solid Earth* **2021**, *126*, e2021JB022775. [CrossRef]
95. Tsatskin, A.; Gendler, T.; Heller, F. Improved Paleopedological Reconstruction of Vertic Paleosols at Novaya Etuliya, Moldova Via Integration of Soil Micromorphology and Environmental Magnetism. In *New Trends in Soil Micromorphology*; Kapur, S., Mermut, A., Stoops, G., Eds.; Springer: Berlin/Heidelberg, Germany, 2008. [CrossRef]

Disclaimer/Publisher's Note: The statements, opinions and data contained in all publications are solely those of the individual author(s) and contributor(s) and not of MDPI and/or the editor(s). MDPI and/or the editor(s) disclaim responsibility for any injury to people or property resulting from any ideas, methods, instructions or products referred to in the content.